

Rollover Cyclometalated Bipyridine Platinum Complexes as Potent Anticancer Agents: Impact of the Ancillary Ligands on the Mode of Action

Maria V. Babak,^{*,†,‡,§} Martin Pfaffeneder-Kmen,^{||} Samuel M. Meier-Menches,[⊥] Maria S. Legina,[†] Sarah Theiner,^{⊥,¶} Cynthia Licona,[▽] Christophe Orvain,[▽] Michaela Hejl,[†] Muhammad Hanif,^{§,||} Michael A. Jakupec,^{†,¶} Bernhard K. Keppler,^{†,¶} Christian Gaiddon,[▽] and Christian G. Hartinger^{*,§,||}

[†]Institute of Inorganic Chemistry, University of Vienna, Waehringer Str. 42, 1090 Vienna, Austria

[‡]Department of Chemistry, National University of Singapore, 3 Science Drive 2, 117543 Singapore

[§]School of Chemical Sciences, University of Auckland, Private Bag 92019, Auckland 1142, New Zealand

^{||}Institute of Physical Chemistry, University of Vienna, Waehringer Str. 42, 1090 Vienna, Austria

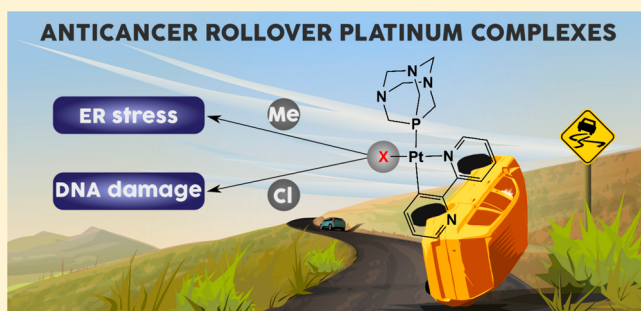
[⊥]Department of Analytical Chemistry, University of Vienna, Waehringer Str. 38, 1090 Vienna, Austria

[¶]Research Cluster Translational Cancer Therapy Research, University of Vienna, 1090 Vienna, Austria

[▽]Inserm UMR_S1113, Signalisation moléculaire du stress cellulaire et pathologies, Université de Strasbourg, 67200 Strasbourg, France

Supporting Information

ABSTRACT: Platinum-based anticancer coordination compounds are widely used in the treatment of many tumor types, where they are very effective but also cause severe side effects. Organoplatinum compounds are significantly less investigated than the analogous coordination compounds. We report here rollover cyclometalated Pt compounds based on 2,2'-bipyridine which are demonstrated to be potent antitumor agents both *in vitro* and *in vivo*. Variation of the co-ligands on the Pt(2,2'-bipyridine) backbone resulted in the establishment of structure–activity relationships. They showed that the biological activity was in general inversely correlated with the reaction kinetics to biomolecules as shown for amino acids, proteins, and DNA. The less stable compounds caused higher reactivity with biomolecules and were shown to induce p53-dependent DNA damage. In contrast, the presence of bulky PTA and PPh₃ ligands was demonstrated to cause lower reactivity and increased antineoplastic activity. Such compounds were devoid of DNA-damaging activity and induced ATF4, a component of the endoplasmic reticulum (ER) stress pathway. The lead complex inhibited tumor growth similar to oxaliplatin while showing no signs of toxicity in test mice. Therefore, we demonstrated that it is possible to fine-tune rollover-cyclometalated Pt(II) compounds to target different cancer pathways and be a means to overcome the side effects associated with cisplatin and analogous compounds in cancer chemotherapy.

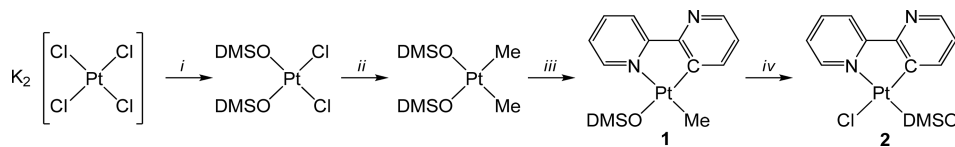


INTRODUCTION

Since cisplatin was introduced into oncological practice in 1978, it has made a significant contribution to the successful treatment of cancer patients. However, its severe side-effects prompted the development of platinum- and other transition-metal-based compounds with improved chemotherapeutic potential.^{1–6} Nowadays, there are numerous chemical libraries of antiproliferative Pt compounds available but only a few drug candidates made their way from bench to clinic.⁷ As the structure of cisplatin contains ammine ligands as nonleaving groups, numerous complexes with ligands with nitrogen donors were prepared, and structure–activity relationships were established.⁸ Several research groups focused on the inves-

tigation of Pt(II) complexes with 2,2'-bipyridine (bipy) and its derivatives.^{9–11} The presence of bipy might result in DNA intercalation of the complex in addition to the covalent platinumation of guanine residues at DNA, establishing a dual DNA-binding mode.^{12,13} Another advantage of bipy is its high lipophilicity which facilitates and improves the cellular uptake and accumulation as compared to cisplatin. Introduction of a 2,2'-bipyridine ligand resulted in significantly increased levels of cell lethality in prostate cancer and melanoma cell lines.^{14,15} In addition, various Pt^{II} complexes with bipy derivatives induced

Received: December 28, 2017

Scheme 1. Synthesis^a of Cyclometalated Pt(II) Complexes with 2,2'-Bipyridine from K₂PtCl₄²⁰

^a(i) DMSO, H₂O, RT; (ii) Sn(CH₃)₄, DMSO, 80 °C; (iii) 2,2'-bipyridine, toluene, 110 °C; (iv) HCl, acetone, DMSO, RT.

apoptosis in cancer cell lines,^{14,15} while the encapsulation of perfluoroalkylated bipy Pt complexes into liposomes did not result in enhanced cytotoxicity.¹⁶ The advantages of using bipy have also been illustrated with other metals, such as Ru-based complexes displaying DNA intercalation¹⁷ or with Os-based complexes inducing higher cytotoxicity that correlates with higher lipophilicity.¹⁸

Typically bipy coordinates to metal centers through the two N donor atoms in a *N,N'*-bidentate fashion.¹⁹ However, under certain conditions, the C–H bond of one pyridine ring might be activated leading to the formation of Pt(II) cyclometalated complexes, where bipy is coordinated in *N,C*-mode (Scheme 1).²⁰ These so-called rollover Pt complexes were discovered by Minghetti et al. in 1999,²¹ and within the past decade they were extensively investigated by Zucca et al.^{22–28}

The research on cyclometalated Pt(II) complexes with anticancer properties has focused on *N,C*-coordinated bipyridine,²⁹ phenylpyridine,^{30–35} COD,³⁶ and other ligands.^{12,13,37–42} These complexes displayed high cytotoxicity in cisplatin-resistant cancer models, interacted with DNA, and several examples showed promising *in vivo* activity.⁴³ *N,C*-coordination seems to have beneficial effects on the biological activity of Pt(II) complexes, probably due to their improved stability and strong Pt–C σ -bond. However, in case of the tridentate *N,C,N'*- and *C,N,N'*-coordinated ligands 1,3-di(2-pyridyl)benzene and 6-phenyl-2,2'-bipyridine, correspondingly, the biological activity was strongly dependent on the coordination pattern at the Pt center and the *trans* effect of the carbon donors.⁴⁴ Based on these observations, we expected that the flipped *N,C*-coordinated bipy ligand in Pt(II) complexes would open the possibility to fine-tune the mechanism of action of the complexes and control their biological activity through the positioning of different ligands *trans* to the carbon or nitrogen atoms of *N,C*-coordinated bipyridine. The release of these ligands would cause a change in charge state and alter the physicochemical properties of the complexes as well as their affinity to biomolecules. Therefore, cyclometalated rollover Pt(II) complexes of *N,C*-coordinated bipyridine were prepared, and studies on their stability, cytotoxicity, cellular accumulation, interactions with biomolecules, effects on protein expression as well as *in vivo* experiments in mouse tumor models are reported.

EXPERIMENTAL SECTION

Materials and Methods. Materials from chemical suppliers were used as received, and all reactions were carried out under argon atmosphere in anhydrous solvents in darkness. The products were isolated without special precautions. 1,3,5-Triaza-7-phosphaadamantane (PTA),⁴⁵ *cis*-[Pt(Me)₂(DMSO)₂],⁴⁶ 1–3, 7, and 8²⁰ were prepared according to literature procedures. Dichloromethane was dried and distilled over CaH₂ under argon atmosphere. Toluene was distilled under argon atmosphere.⁴⁷ 2,2'-Bipyridine was purchased from Alfa Aesar, dimethyl sulfoxide, guanosine-5'-triphosphate, ubiquitin (bovine erythrocytes) and horse heart cytochrome C from Sigma, *tert*-butyl isocyanide, adenosine-5'-triphosphate from Calbio-

chem and *L*-methionine from Sigma-Aldrich, methanol (HPLC grade) from Fisher, formic acid, *L*-glutamic acid, and *L*-cysteine from Fluka, and *L*-histidine from Merck. Milli-Q water was taken from an Advantage A10 (18.2 M Ω , 185 UV Ultrapure water system, Millipore, Molsheim, France). Elemental analyses were performed by the Microanalytical Laboratory of the Faculty of Chemistry of the University of Vienna. The ¹H, ³¹P, ¹⁹⁵Pt NMR spectra were recorded at 500.10, 202.44, and 107.33 MHz, respectively, on a Bruker FT NMR spectrometer Avance II 500 MHz. Chemical shifts are given in parts per million (ppm) relative to the residual solvent peak.

The X-ray intensity data were measured on Bruker D8 Venture diffractometer equipped with multilayer monochromator, Mo–K α INCOATEC micro focus sealed tube and Kryoflex cooling device. The structure was solved by direct methods and refined by full-matrix least-squares techniques. Non-hydrogen atoms were refined with anisotropic displacement parameters. Hydrogen atoms were inserted at calculated positions and refined with a riding model. The following software was used: Bruker SAINT software package⁴⁸ using a narrow-frame algorithm for frame integration, SADABS⁴⁹ for absorption correction, OLEX2⁵⁰ for structure solution, refinement, molecular diagrams, and graphical user-interface, Shelxle⁵¹ for refinement and graphical user-interface SHELXS-2013⁵² for structure solution, SHELXL-2013⁵³ for refinement, and Platon⁵⁴ for symmetry check, molecular diagrams, Mercury 3.0. Experimental data and CCDC codes can be found in Table S1.

Cell Lines and Culture Conditions. CH1(PA-1) cells (identified via STR profiling as PA-1 ovarian teratocarcinoma cells by Multiplexion, Heidelberg, Germany; compare Korch et al.⁵⁵) were obtained from Lloyd R. Kelland, CRC Centre for Cancer Therapeutics, Institute of Cancer Research, Sutton, U.K. A549 (human non-small cell lung cancer) and SW480 (human colon carcinoma) cells were supplied by Brigitte Marian (Institute of Cancer Research, Department of Medicine I, Medical University of Vienna, Austria). HCT116 human colon cancer cells were obtained from ATCC. All cell culture media and reagents were purchased from Sigma-Aldrich, Austria, unless noted otherwise, and plastic ware was obtained from Starlab, Germany. Adherent cell cultures were grown in 75 cm² culture flasks in complete medium [i.e., minimal essential medium (MEM) supplemented with 10% heat-inactivated fetal bovine serum (Invitrogen), 1 mM sodium pyruvate, 4 mM *L*-glutamine, and 1% v/v nonessential amino acids from 100 \times ready-to-use stock]. HCT116 cell line was cultured in Dulbecco's modified minimal essential medium (DMEM) containing 10% fetal bovine serum (Dominique Dutcher) and 1% penicillin + streptomycin (Sigma). All cell lines were grown at 37 °C in a humidified atmosphere of 95% air and 5% CO₂. Experiments were performed on cells within 20 passages.

Cytotoxicity Assay in Cancer Cell Lines. The cytotoxicity of the compounds was determined by means of a colorimetric microculture assay (MTT assay, MTT = 3-(4,5-dimethyl-2-thiazolyl)-2,5-diphenyl-2H-tetrazolium bromide). The cells were harvested from culture flasks by trypsinization and seeded in densities of 1 \times 10³ [CH1(PA-1)], 2 \times 10³ (SW480), 3 \times 10³ (A549), and 5 \times 10³ cells (for HCT116) in 100 μ L/well aliquots in 96-well microculture plates. After the cells were allowed to resume exponential growth for 24 h, the test compounds were dissolved in DMSO, then diluted in MEM, and added to the plates where the final DMSO content did not exceed 0.5%. After exposure for 96 h (48 h in case of HCT116), drug solutions were replaced with 100 μ L/well of a 1/7 MTT/RPMI 1640 solution (MTT solution, 5 mg/mL of MTT reagent in phosphate-buffered saline; RPMI 1640 medium, supplemented with 10% heat-inactivated fetal

bovine serum and 4 mM L-glutamine). All manipulations with HCT116 cells were performed in DMEM. After incubation for 4 h at 37 °C, the MTT/RPMI 1640 or MTT/DMEM mixtures were removed, and the formazan crystals formed in viable cells were dissolved in 150 μ L of DMSO per well. Optical densities were measured at 550 nm with a microplate reader (Biotek ELx808), by using a reference wavelength of 690 nm to correct for unspecific absorption. The quantity of viable cells was expressed in terms of treated/control (T/C) values by comparison to untreated control microcultures, and 50% inhibitory concentrations (IC_{50}) were calculated from concentration–effect curves by interpolation. Evaluation was based on means from at least three independent experiments, each comprising three replicates per concentration level.

Cellular Accumulation. Studies on the cellular accumulation of complexes 1–4 were performed in comparison to cisplatin according to a previously described procedure.⁵⁶ SW480 cells were seeded in 6-well plates at densities of 1.2×10^5 cells per well in aliquots of 2.5 mL MEM. Accumulation experiments and corresponding adsorption/desorption controls were located on the same plate, and an additional plate included controls for cell counting. Plates were kept at 37 °C for 24 h prior to addition of the respective complex. Cells were incubated with the compounds at concentrations of 50 μ M for 2 h at 37 °C. Afterward, the medium was removed, and cells were washed three times with PBS and lysed with 0.5 mL subboiled HNO_3 per well for 1 h at room temperature. Lysates were diluted with Milli-Q water resulting in nitric acid concentrations lower than 3% and platinum concentrations lower than 15 μ g/g. The total platinum content was determined with an ICP-quadrupole MS Agilent 7500ce (Agilent Technologies, Waldbronn, Germany). The adsorption/desorption blank data were subtracted from the data for the corresponding accumulation sample, and the platinum content was referred to the cell number. The results are based on at least three independent experiments, each consisting of three replicates. The ICP-MS instrument was equipped with a CETAX ASX-520 autosampler (Nebraska, USA) and a MicroMist nebulizer operating at a sample uptake rate of approximately 0.25 mL/min. The instrument was tuned on a daily base in order to achieve maximum sensitivity. Platinum and rhenium standards were obtained from CPI International (Amsterdam, The Netherlands). Rhenium served as the internal standard for platinum to account for instrumental fluctuations and matrix effects. Quantification was done using the isotopes ^{185}Re and ^{195}Pt with a dwell time of 0.3 s and 10 replicates. The ICP-MS instrument was equipped with nickel cones and was operated at an RF power of 1550 W. Argon was used as plasma (15 L/min) and carrier gas with a flow rate of ~ 1.1 L/min. The Agilent MassHunter software package (Workstation Software, Version B.01.01, 2012) was used for data processing.

Interactions with DNA. A 500 ng portion of plasmid DNA pUC19 (2686 bp; Fermentas Life Sciences) was incubated with 50 μ M of the test compounds in a 0.1 \times Tris-EDTA (TE) buffer for time intervals of 5, 15, 30, 60, 120, and 240 min at 37 °C. Electrophoresis was performed in a 1% agarose gel (Sigma-Aldrich) in 1 \times Tris-borate-EDTA (TBE) buffer for 90 min at 80 V. Gels were stained with ethidium bromide in 1 \times TBE (0.75 μ g/mL) for 20 min. Images were taken with the detection system Fusion SL (Vilber Lourmat). Three independent experiments were performed.

Protein Extraction and Western Blot. HCT116 cells were grown on Cellstar 6-well plates (Greiner Bio-One) and treated at 37 °C and 5% CO_2 for 24 h with 1, 3–5 at their respective IC_{50} and IC_{75} concentrations as well as oxaliplatin and tunicamycin at their IC_{50} concentrations. The cells were lysed with lysis buffer [100 μ L, 1% NP40, 150 mM NaCl, 50 mM Tris-HCl (pH 8.0), protease inhibitor]. The cell lysate was transferred to individual 2 mL tubes and sonicated for 10 s. The samples were then centrifuged at 13,000 rpm and 4 °C for 15 min. The supernatant liquid containing the proteins was collected, and the total protein content of each sample was quantified via Bradford's assay. Forty μ g of protein from each sample were reconstituted in loading buffer (5% DDT, 1 \times protein loading dye) and heated at 95 °C for 5 min. The protein mixtures were resolved on a 10% SDS-PAGE gel by electrophoresis and transferred to a

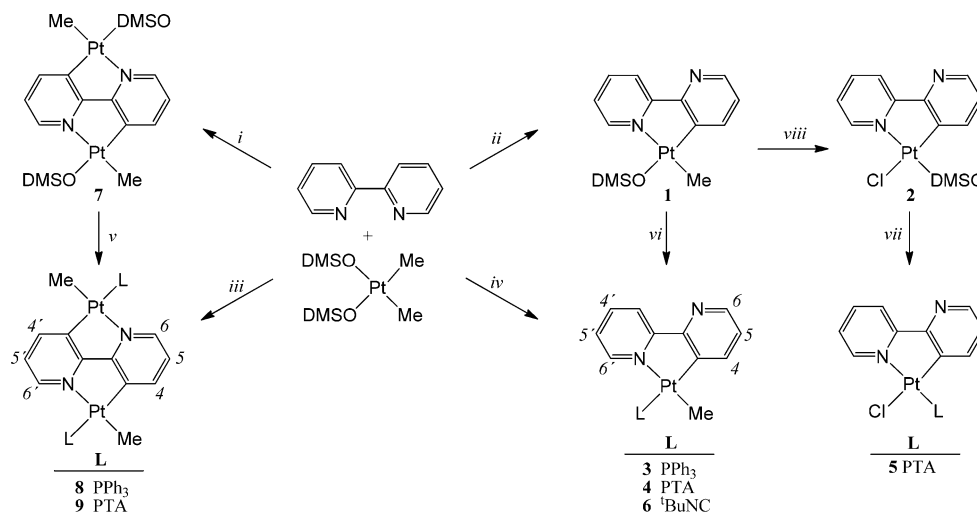
nitrocellulose membrane. Equal loading of protein was confirmed by comparison with actin. Immunoblotting was done with anti-p53 (rabbit anti-p53, FL-393, Santa Cruz, CA), anti-ATF4 (anti-CREB-2 (B-3): sc-390063), and antiactin (rabbit anti- β -actin, Sigma) antibodies. The protein bands were visualized via enhanced chemiluminescence imaging (PXi, Syngene).

Animal Studies. The toxicity studies were performed in female Balb/C mice. Complex 1 was administered intraperitoneally to three groups of mice (3 mice per group) every 4 days over 12 days, and after that the mice were observed for 8 days. Mice in group 1 were injected with a drug dose of 4 μ mol/kg on days 1 and 4 and 15 μ mol/kg on days 8 and 12. Mice in group 2 were injected with a drug dose of 8 μ mol/kg on days 1 and 4 and 12 μ mol/kg on days 8 and 12. Mice in group 3 were injected with 10 μ mol/kg only on days 1, 4, and 8. Mouse survival and body weight variations were monitored daily for 20 days in all groups. The maximum tolerated dose (MTD) was defined as the highest dose that induced no more than 15% weight loss vs control, caused no toxic death, and was not associated with remarkable changes in vital signs within a week after administration.

The *in vivo* antitumor effect of the drug of interest was evaluated in the Balb/C syngeneic CT26 tumor model. CT26 mouse colon cancer cells (1×10^5 cells) were implanted subcutaneously in 8 weeks-old Balb/C mice ($n = 8$). When tumors reached 150 mm³, mice were injected intraperitoneally with oxaliplatin (25 μ mol/kg) or compound 1 (18 μ mol/kg) twice a week (on days 1 and 4). Tumor sizes were monitored using a caliper, and body weight was measured daily for toxicity evaluation. The stock solution of 1 was prepared in DMSO and subsequently diluted with hydrogenated castor oil Cremophor and PBS. The solubility of complexes 3, 4, and 5 in Cremophor was not sufficient for the *in vivo* studies. Statistical analysis was done by the two-tail ANOVA test with Bonferroni post-test using GraphPad Prism software (GraphPad Software Inc., CA) with $P < 0.05$ considered as significant (* $p < 0.05$, *** $p < 0.001$).

NMR- and MS-Based Biomolecule Interaction Studies. NMR and mass spectrometric (MS) methods were employed to characterize the adduct formation of the Pt complexes with biomolecules such as amino acids, nucleotides, and proteins. For NMR experiments, a solution of 4 (1 mg/mL) in [D₆]DMSO/D₂O (5/95) was treated with 2 equiv of Cys, His and Met, and 1H and ^{31}P { 1H } NMR spectra were recorded after 30 min, 1, 3, 24, 48, and 72 h on a Bruker DRX 400 MHz NMR spectrometer at measurement frequencies of 400.13 (1H), and 161.98 MHz (^{31}P { 1H }) at ambient temperature. For MS experiments, stock solutions of 2 (1% DMSO, 100 μ M), 1 and 4 (1% DMSO, 400 μ M) and mixtures of amino acids (Met, His, Cys and Glu, each 400 μ M), nucleic acids (ATP and GTP, each 400 μ M) and proteins (ub and cyt, each 400 μ M) were prepared in water. The complexes were incubated with the proteins in water in the dark at 37 °C at a metal concentration of 50 μ M. The reaction mixtures with the amino acids (1:1:1:1 metal-to-amino acid ratio) and the nucleic acids (1:1:1 metal-to-NTP ratio) were prepared analogously. Additionally, the same compounds were incubated with a mixture of ubiquitin (ub) and cytochrome C (cyt) at a 1:1:1 metal-to-protein ratio. Mass spectra of the incubation mixtures were recorded after 2 and 24 h on an electrospray ionization trap-mass spectrometer (ESI-IT-MS) and additionally on an ESI-time-of-flight (TOF) MS for the protein incubation after 48 h. Samples were diluted to 5 μ M metal or protein content with water or water:methanol:formic acid (50:50:0.2), respectively.

ESI-IT-mass spectra were recorded on an AmaZon SL ion trap mass spectrometer (Bruker Daltonics GmbH, Bremen, Germany) by direct infusion at a flow rate of 4–5 μ L/min. The instrument parameters were as follows: 77% RF level, average accumulation time 3 ms (ESI⁺) and 14 ms (ESI⁻), scan range m/z 100–2200, 64.7 trap drive, -4.5 kV capillary voltage, -0.5 kV end plate offset, 180 °C dry temperature, 8 psi nebulizer, 6 L/min dry gas. Mass spectra were recorded over 0.5 min and averaged in positive and negative ion modes. Data were processed using DataAnalysis 4.0 (Bruker Daltonics GmbH, Bremen, Germany). The protein spectra were deconvoluted using the maximum entropy deconvolution algorithm with automatic data point spacing and 0.5 instrument peak width. Samples containing

Scheme 2. Synthesis of Mono- And Dinuclear Cyclometalated 2,2'-Bipyridine Pt(II) Complexes^a

^a(i–iv) L, toluene, 110 °C; (v–vii) L, dichloromethane, RT; (viii) HCl, acetone, RT.

proteins were additionally analyzed on a Maxis UHR-TOF (Bruker Daltonics GmbH, Bremen, Germany) in positive ion mode. The instrument was equipped with a Triversa nanomate (Advion Biosystems Inc., Ithaca, New York, USA) using the ChipSoft 8.3 software for Chip control (Advion Biosystems Inc.). The instrument parameters were as follows: Ion cooler RF 280 Vpp, ion cooler transfer time 150 μ s, scan range m/z 100–2000, gas flow 0.1 psi, dry heater 180 °C, HV capillary –1.8 kV. Data was processed using DataAnalysis 4.0 (Bruker Daltonics GmbH, Bremen, Germany). Protein spectra were deconvoluted using the maximum entropy deconvolution algorithm with automatic data point spacing and 30,000 instrument resolving power.

Synthesis of Complexes. *[Pt(bipy)(PTA)(Me)] (4).* *Method 1.* The synthetic method was adapted from a literature procedure.²⁰ PTA (16 mg, 0.1 mmol, 1 equiv) was added to a solution of [Pt(DMSO)(bipy)(Me)] (46 mg, 0.1 mmol) in anhydrous CH₂Cl₂ (20 mL). The pale yellow solution was stirred for 2 h, filtered, and concentrated under reduced pressure to ca. 2 mL. The product was precipitated by slow addition of cold hexane (ca. 50 mL), filtered, washed with hexane, and dried *in vacuo* to get 27 mg of yellow powder. Yield: 52%.

Method 2. The synthetic method was adapted from a literature procedure.²⁵ 2,2'-Bipyridine (94 mg, 0.6 mmol) and *cis*-[Pt(Me)₂(DMSO)₂] (127 mg, 0.3 mmol) were dissolved in anhydrous toluene (10 mL) and heated to reflux for 3 h. The color of the solution slowly changed from red to yellow. PTA (56 mg, 0.4 mmol, 1.2 equiv) was added to the solution, and the color of the solution immediately changed to pale yellow. The solution was refluxed for 1 h and then cooled down to room temperature. The reaction mixture was concentrated to a small volume, the residue was extracted with water, and organic phase was quickly separated and dried with Na₂SO₄. The solution was filtered and concentrated to a small volume. The product was precipitated by slow addition of cold hexane (ca. 50 mL), filtered, washed with hexane, and dried *in vacuo* to get 96 mg of yellow microcrystals. Yield: 61%. The product can be additionally purified by slow diffusion of diethyl ether into dichloromethane solution, resulting in the formation of yellow crystals.

Elemental analysis (%) calcd for C₁₇H₂₂N₅Pt (522.44 g mol⁻¹): C 39.08, H 4.24, N 13.41; found: C 38.93, H 4.30, N 13.15; ¹H NMR (500.10 MHz; [D₆]DMSO): δ = 8.70 ppm (d with broad ¹⁹⁵Pt satellites, 1H, ³J_{H–H} = 5.4 Hz, ³J_{Pt–H} = 14 Hz, H_{6'}), 8.30 (d, 1H, ³J_{H–H} = 4.8 Hz, H₆), 8.23 (dd, 1H, ³J_{H–H} = 7.9 Hz, ⁴J_{H–H} = 0.9 Hz, H₃), 8.15 (td, 1H, ³J_{H–H} = 8.3 Hz, ⁴J_{H–H} = 0.9 Hz, H_{4'}), 7.96 (ddd with ¹⁹⁵Pt satellites, 1H, ³J_{H–H} = 7.7 Hz, ⁴J_{H–H} = 5.4 Hz, ⁴J_{Pt–H} = 1.6 Hz, ³J_{Pt–H} = 48 Hz, H₄), 7.53 (ddd, 1H, ³J_{H–H} = 7.7 Hz, ³J_{H–H} = 5.6 Hz, ⁴J_{H–H} = 1.6 Hz, H₅), 7.21 (ddd, 1H, ³J_{H–H} = 7.7 Hz, ³J_{H–H} = 4.6 Hz, ⁵J_{Pt–H} =

1.8 Hz, H₅), 4.55 (d, 3H, ²J_{H–H} = 12.6 Hz, P(CHH)₃), 4.45 (d, 3H, ²J_{H–H} = 12.6 Hz, P(CHH)₃), 4.26 (s, 6H, (NCH₂)₃), 0.74 (d with ¹⁹⁵Pt satellites, 3H, ³J_{Pt–H} = 7.6 Hz, ²J_{Pt–H} = 83.0 Hz, CH₃); ³¹P NMR (202.44 MHz, [D₆]DMSO): δ = –67.0 (s with ¹⁹⁵Pt satellites, ¹J_{Pt–P} = 1964 Hz, P(CH₂)₃); ¹⁹⁵Pt NMR (107.33 MHz, [D₆]DMSO): δ = –2536 ppm (d, ¹J_{Pt–P} = 1948 Hz).

[Pt(bipy)(PTA)Cl] (5). The synthetic method was adapted from a literature procedure.²⁰ PTA (16 mg, 0.1 mmol, 1 equiv) was added to a solution of [Pt(DMSO)(bipy)Cl] (46 mg, 0.1 mmol) in anhydrous CH₂Cl₂ (20 mL). The pale yellow solution was stirred for 2 h, filtered, and concentrated under reduced pressure to ca. 2 mL. The product was precipitated by slow addition of cold hexane (ca. 50 mL), filtered, washed with hexane, and dried *in vacuo* to get 31 mg of light yellow powder. Yield: 57%.

Elemental analysis (%) calcd for C₁₆H₁₉N₅PtCl (542.86 g mol⁻¹): C 35.40, H 3.53, N 12.90, P 5.71; found: C 35.24, H 3.39, N 12.83, P 5.68; ¹H NMR (500.10 MHz; [D₆]DMSO): δ = 9.44 ppm (m, 1H, H_{6'}), 8.36 (dd, 1H, ³J_{H–H} = 4.6 Hz, ⁴J_{H–H} = 1.2 Hz, H₆), 8.23–8.17 (m, 2H, H₃, H_{4'}), 7.91 (d with ¹⁹⁵Pt satellites, 1H, ³J_{H–H} = 7.6 Hz, ³J_{Pt–H} = 54 Hz, H₄), 7.71 (td, 1H, ³J_{H–H} = 5.6 Hz, ⁴J_{H–H} = 2.7 Hz, H₅), 7.14 (dd, 1H, ³J_{H–H} = 7.8 Hz, ³J_{H–H} = 4.6 Hz, H₅), 4.61 (d, 3H, ²J_{H–H} = 12.5 Hz, P(CHH)₃), 4.47 (d, 3H, ²J_{H–H} = 12.5 Hz, P(CHH)₃), 4.45 (s, 6H, (NCH₂)₃). ³¹P NMR (202.44 MHz, [D₆]DMSO): δ = –66.6 (s with ¹⁹⁵Pt satellites, ¹J_{Pt–P} = 3780 Hz, P(CH₂)₃); ¹⁹⁵Pt NMR (107.33 MHz, [D₆]DMSO): δ = –2528 ppm (d, ¹J_{Pt–P} = 3794 Hz).

[Pt(bipy)(BuNC)(Me)] (6). BuNC (11 μ L, 0.1 mmol, 1 equiv) was added to a solution of [Pt(DMSO)(bipy)(Me)] (46 mg, 0.1 mmol) in anhydrous CH₂Cl₂ (20 mL). The pale yellow solution was stirred for 2 h, filtered, and concentrated under reduced pressure to ca. 2 mL. The product was precipitated by slow addition of cold hexane (ca. 50 mL), filtered, washed with hexane, and dried *in vacuo* to get light yellow film (3 mg). Yield: 15%.

Elemental analysis (%) calcd for C₁₆H₁₉N₅Pt (448.42 g mol⁻¹): C 42.86, H 4.27, N 9.37; found: C 42.74, H 4.33, N 9.28; ¹H NMR (500.10 MHz; [D₆]DMSO): δ = 8.77 ppm (d with ¹⁹⁵Pt satellites, 1H, ³J_{H–H} = 5.4 Hz, ³J_{Pt–H} = 15 Hz, H₆), 8.29 (dd, 1H, ³J_{H–H} = 4.6 Hz, ⁴J_{H–H} = 1.6 Hz, H₆), 8.21 (dd, 1H, ³J_{H–H} = 7.8 Hz, ⁴J_{H–H} = 1.0 Hz, H₃), 8.16 (td, 1H, ³J_{H–H} = 8.0 Hz, ⁴J_{H–H} = 1.2 Hz, H_{4'}), 7.91 (dd with ¹⁹⁵Pt satellites, 1H, ³J_{H–H} = 7.4 Hz, ⁴J_{H–H} = 1.7 Hz, ³J_{Pt–H} = 47 Hz, H₄), 7.55 (ddd, 1H, ³J_{H–H} = 7.2 Hz, ³J_{H–H} = 5.6 Hz, ⁴J_{H–H} = 1.8 Hz, H₅), 7.19 (dd, 1H, ³J_{H–H} = 7.5 Hz, ³J_{H–H} = 4.7 Hz, H₅), 1.61 (s, 6H, BuNC), 0.85 (s with ¹⁹⁵Pt satellites, 3H, ²J_{Pt–H} = 86.0 Hz, CH₃); ¹⁹⁵Pt NMR (107.33 MHz, [D₆]DMSO): δ = –2381 ppm (s).

[(bipy)(Pt(PTA)(Me))₂] (9). The synthetic method was adapted from a literature procedure.²⁰ PTA (20 mg, 0.128 mmol, 2 equiv) was added

to a solution of $[(\text{bipy})(\text{Pt}(\text{DMSO})(\text{Me}))_2]$ (47 mg, 0.064 mmol) in anhydrous CH_2Cl_2 (20 mL). Several minutes after PTA addition, a yellow precipitate formed. The suspension was stirred for 2 h and filtered. The solid was washed with diethyl ether and dried *in vacuo* to give 37 mg of pale yellow solid. Yield: 65%

Elemental analysis (%) calcd for $\text{C}_{24}\text{N}_6\text{H}_{36}\text{P}_2\text{Pt}_2\cdot\text{H}_2\text{O}\cdot 0.5\text{CH}_2\text{Cl}_2$ (888.70 g mol⁻¹): C 31.00, H 4.14, N 11.81; found: C 31.30, H 4.05, N 11.60. ¹H NMR (500.10 MHz; CDCl_3): δ = 8.19 (ddd with ¹⁹⁵Pt satellites, 2H, ³*J*_{H-H} = 7.7 Hz, ⁴*J*_{H-H} = 2.1 Hz, ⁴*J*_{P-H} = 6.4 Hz, ²*J*_{Pt-H} = 45 Hz, *H*_{4/4'}), 8.10 (d, 2H, ³*J*_{H-H} = 5.2 Hz, *H*_{6/6'}), 7.11 (ddd, 2H, ³*J*_{H-H} = 7.6 Hz, ³*J*_{H-H} = 5.4 Hz, ⁵*J*_{P-H} = 2.1 Hz, *H*_{5/5'}), 4.63 (d, 6H, ²*J*_{H-H} = 13.1 Hz, *P*(*CHH*)₃), 4.58 (d, 6H, ²*J*_{H-H} = 13.1 Hz, *P*(*CHH*)₃), 4.33 (s, 12H, (*NCH*)₃), 0.84 (d with ¹⁹⁵Pt satellites, 3H, ³*J*_{P-H} = 7.6 Hz, ²*J*_{Pt-H} = 80.0 Hz, *CH*₃); ³¹P NMR (202.44 MHz, CDCl_3): δ = -65.4 (s with ¹⁹⁵Pt satellites, ¹*J*_{Pt-P} = 2050 Hz, ¹*P*(*CH*)₃); ¹⁹⁵Pt NMR (107.33 MHz, CDCl_3): δ = -2448 ppm (d, ¹*J*_{Pt-P} = 2095 Hz).

RESULTS AND DISCUSSION

The C–H bond in bipy may be activated upon interaction with *cis*-[Pt(Me)₂(DMSO)₂] at 110 °C in anhydrous toluene under inert atmosphere.²⁰ Depending on the ratio of Pt complex and bipyridine, the mononuclear complex **1** (1:1 ratio) or dinuclear **7** (2:1 ratio) can be obtained (Scheme 2).²⁰ Both complexes allow for substitution of the *S*-bound DMSO ligand, which occupies a *trans* position to the C3 atom coordinated to the Pt center, with triphenylphosphine (complexes **3** and **8**) and other 2e⁻ donors. The structurally related mono- and dinuclear 1,3,5-triaza-7-phosphaadamantane (PTA) complexes **4** and **9** were prepared in moderate yields of 52 and 65%, respectively, by stirring **1** and **7** in dichloromethane with PTA for 2 h. Complex **6** with a *C*-coordinated *tert*-butyl isocyanide was synthesized in a similar way, but the yield was unsatisfactory (15%). Alternatively, complexes **4** and **9** were obtained from one-pot reactions starting from *cis*-[Pt(Me)₂(DMSO)₂] and bipy in toluene,²⁵ which does not require tedious isolation of intermediate DMSO complexes. It should be noted that PTA was added to the reaction mixture in a strictly stoichiometric amount, because addition of PTA in excess resulted in the formation of poorly soluble Pt species with three PTA ligands (as detected by mass spectrometry, data not shown), which could not be separated from the target product.

Complexes **1**–**9** were characterized by NMR spectroscopy and elemental analysis. The aromatic regions in the ¹H NMR spectra ([D6]DMSO) of the mononuclear complexes **4** and **5** revealed seven well-separated resonances with two proton signals flanked by ¹⁹⁵Pt satellites (³*J*_{Pt-H} ≈ 47 Hz for *H*₄ and ³*J*_{Pt-H} ≈ 14 Hz for *H*₆). This is in agreement with the cyclometalated nature of the Pt complex and literature data.²⁰ The chemical shifts of the bipy protons do not depend on the chemical nature of the ligand in *trans* position with the exception of *H*₄ and *H*₆, which are proximate to the Pt center. The methylate group in **4** is represented by a doublet with ¹⁹⁵Pt satellites (δ 0.74 ppm, ³*J*_{P-H} = 8 Hz, ²*J*_{Pt-H} = 83 Hz) which is consistent with its *trans* position to the nitrogen atom and being *cis* to the phosphorus atom of PTA. Due to the absence of a phosphorus atom in **6**, the methyl group is represented by a singlet with ¹⁹⁵Pt satellites at δ 0.85 ppm (³*J*_{Pt-H} = 86 Hz). In contrast to PTA complexes,^{39,57} where the PTA ligand is usually represented by two singlets (*CH*₂ groups of upper and lower rims of adamantane), three signals were assigned to PTA in **4**, that is, two signals for the diastereotopic *P*–*CH*₂–*N* protons at 4.55 and 4.45 ppm and one signal for the *N*–*CH*₂–*N* protons at 4.26 ppm. Additionally, ³¹P and ¹⁹⁵Pt NMR

spectra of **4** revealed strong *P*–*Pt* coupling (¹*J*_{Pt-P} ≈ 1948 Hz; compare the ³¹P and ¹⁹⁵Pt NMR signals for **1**–**9** listed in Table S2).

The stability of **3** and **4** in chloroform, dimethylformamide, and dimethyl sulfoxide was monitored by NMR spectroscopy. While ¹H NMR spectra of the complexes in [D6]DMSO and [D7]DMF remained unchanged for 24 h of measurements, in CDCl_3 gradual decomposition of the complexes was observed after several hours with the appearance of additional sets of signals in ¹H and ³¹P NMR spectra. The ¹H NMR spectrum recorded in CDCl_3 of the dinuclear PTA complex **9** is similar to those of **7** and **8** but markedly different from that of the mononuclear analogue **4**. The aromatic region featured only three signals which supports the symmetric dinuclear structure of the complex. Similarly to mononuclear **4**, the PTA *P*–*CH*₂–*N* protons were detected as two doublets at 4.63 and 4.58 ppm, whereas the PTA *N*–*CH*₂–*N* protons were identified as a singlet at 4.33 ppm. The methyl groups were observed at 0.84 ppm as a doublet flanked by ¹⁹⁵Pt satellites (³*J*_{P-H} = 8 Hz, ²*J*_{Pt-H} = 80 Hz).

The methylato ligand in cyclometalated bipy complexes can be substituted by a chlorido ligand, and such Me/Cl exchange is accompanied by displacement of DMSO from *trans* to a *cis* position with respect to the coordinated carbon atom of bipy (**1** and **2**, Scheme 1).⁵⁸ Thus, contrary to **4** and **9**, the PTA ligand in **5** was found in *trans* position to the coordinated nitrogen atom of bipy. As a result, the *H*₆ proton resonated in NMR spectra ([D6]DMSO) downfield at 9.44 vs 8.70 ppm, and the ¹*J*_{Pt-Pt} coupling constant was significantly higher at 1948 and 3794 Hz for **4** and **5**, correspondingly, which was previously observed for structurally related triphenylphosphine complexes.²⁰

The molecular structures of complexes **4**· CH_2Cl_2 and **5** were confirmed by X-ray diffraction analysis (Figure 1, selected bond distances and angles are listed in Table 1) and compared to that of **3**⁵⁹ and [Pt(bipy)(PPh₃)Cl].²⁰

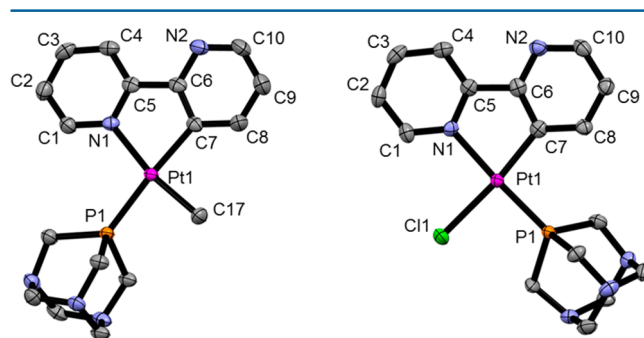


Figure 1. Molecular structures of **4**· CH_2Cl_2 (left) and **5** (right) drawn at 50% probability level. Solvent molecules and hydrogen atoms were omitted for clarity.

The coordination geometry around the metal center in the Pt complexes is slightly distorted from a square-planar environment, which is in agreement with previously published structural data on Pt cyclometalated complexes.^{20,40} The angles around the Pt center deviate from 90° with the smallest values for the C7–Pt1–N1 angle (79.61(9)° in **3**,⁵⁹ 79.66(7)° in **4**, and 80.55(9)° in **5**) and the biggest values found between the phosphorus-containing ligand and the pyridine ring (97.91(6)° and 103.95(5)° for N1–Pt1–P1 in **3** and **4**, correspondingly, and 96.57(7)° for C7–Pt1–P1 in **5**). This may be explained by

Table 1. Key Bond Lengths (Å) and Angles (deg) Observed in the Molecular Structures of **4** and **5** in Comparison with **3**⁵⁹ and [Pt(bipy)(PPh₃)Cl]²⁰

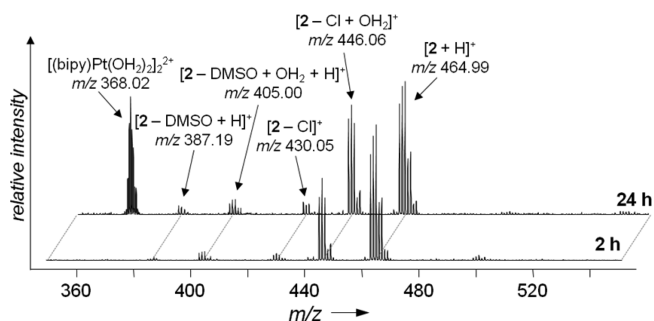
bond lengths (Å) and angles (deg)	3	4	5	[Pt(bipy)(PPh ₃)Cl]
Pt1–C7	2.043(3)	2.049(2)	1.997(2)	2.002(3)
Pt1–P1	2.2904(7)	2.2772(5)	2.2123(6)	2.228(1)
Pt1–N1	2.130(2)	2.1183(17)	2.100(2)	2.091(2)
Pt1–CH ₃	2.077(4)	2.062(2)	–	–
Pt1–Cl1	–	–	2.3908(6)	2.379(1)
C7–Pt1–CH ₃	91.65(11)	90.08(8)	–	–
C7–Pt1–N1	79.61(9)	79.66(7)	80.55(9)	80.82(9)
H ₃ C–Pt1–N1	169.26(1)	169.74(7)	–	–
C7–Pt1–P1	173.67(7)	175.92(6)	96.57(7)	94.68(8)
H ₃ C–Pt1–P1	91.41(8)	86.30(6)	–	–
N1–Pt1–P1	97.91(6)	103.95(5)	174.71(6)	171.86(5)
C7–Pt1–Cl1	–	–	173.53(7)	171.59(7)
N1–Pt1–Cl1	–	–	93.23(6)	91.51(6)
P1–Pt1–Cl1	–	–	89.77(2)	93.35(2)

the constraint of the five-membered ring and the steric demands of the bulky PTA and PPh₃ ligands. The C–N distances in bipy are shorter than the C–C bonds and do not significantly vary from each other in all complexes. The longest distance in bipy was assigned to C5–C6 (1.477(3), 1.476(3), and 1.471(3) Å in **3**, **4**, and **5**, correspondingly) and the shortest bond length to N2–C10 (1.336(3), 1.337(3) and 1.339(3) Å in **3**, **4** and **5**, respectively). However, due to the shift of PTA from a *trans* position to C7 in **4** to *trans* to N1 in **5** and the stronger *trans* influence of the carbon atom than that of the nitrogen atom, the Pt1–P1 distance in **4** (2.2772(5) Å) is significantly longer than in **5** (2.2123(6) Å). For the same reason, the Pt1–Cl1 distance (2.3908(8) Å) is markedly longer than Pt1–CH₃ (2.062(2) Å). In the structurally related complex dichloro(*N*-methyl-2,2'-bipyridylum)platinum(II) Pt–Cl bond lengths of 2.301(3) and 2.396(3) Å were reported for the chlorido ligands in *trans* position to the N and C atoms of *N*-methyl-2,2'-bipyridylum, respectively.⁶⁰ The values for complex **5** are in good agreement with the values reported for complex Pt(bipy)(PPh₃)Cl.²⁰ Notably, in all structures the rotation of one pyridine ring brings N2 close to H4, with N2...H4 distances of 2.574, 2.576, and 2.617 Å in **3**–**5**, correspondingly.

Stability and Identification of Reactive Species in Solution. Pt(II) anticancer drugs usually act as prodrugs and require activation through ligand exchange reactions in the biological medium. In cyclometalated Pt(II) complexes, the stronger Pt–L bond is known to be associated with higher biological activity.¹² It was shown that neutral ligands which remain bound to a Pt center in aqueous solution (i.e., PPh₃, P(OMe)₃, 2,6-dimethylpyridine) enhance the antiproliferative effect of the complexes in comparison with compounds where L is quickly released (i.e., *S*-DMSO, NH₃).¹² In order to evaluate the relationship between the behavior of the complexes in aqueous media and their biological activity, stability studies of complexes **1**, **2**, and **4** were performed by means of ESI-MS (see Table S3 for the experimental and theoretical mass signals).

After 2 h of dissolution in water, the mass spectra recorded for the chlorido complex **2** featured several signals in addition to the most abundant peak assigned to the pseudo molecular ion [2 + H]⁺ (*m/z* 464.99), which remained the most abundant signal for up to 24 h. The complex seems to be activated according to the classical scheme of square-planar Pt^{II}

complexes by hydrolyzing the Pt–Cl bond and forming the aqua complex [(bipy-κ²N,C)Pt(DMSO) + H₂O]⁺ (*m/z* 446.06, Figure 2). In addition, release of DMSO with a concurrent

**Figure 2.** ESI-IT mass spectra of **2** in water after 2 and 24 h.

retention of the chlorido ligand was also observed by the formation of [(bipy-κ²N,C)PtCl + H]⁺ (*m/z* 387.19) and [(bipy-κ²N,C)PtCl + H₂O + H]⁺ (*m/z* 405.00). The hydrolysis pathway seems to terminate in a dimeric species corresponding to an aqua-bridged dimer of the form [(bipy-κ²N,C)Pt(μ-H₂O)]₂²⁺ (*m/z* 368.02), implying that both the chlorido and the DMSO ligands are ultimately exchanged by aqua ligands. Hydrolysis may therefore occur either via release of the chlorido or the DMSO ligands for **2**.

Replacing the chlorido by a methylato ligand as in **1** and **4** leads to increased resistance to hydrolysis. No significant changes were observed in their mass spectra during the 24 h incubation period, as was also shown for **4** by NMR spectroscopy (Figure S1). The most abundant signal of **4** was assigned to [4 + H]⁺ (*m/z* 523.10), while [1 – CH₃ + OCH₃]⁺ (*m/z* 460.01) was most abundant for **1**. The mass signal assigned to [4 + OH]⁺ was also detected for **4** (Figure S2). This suggests that the reaction pathways of the methylato complexes may occur via an associative pathway. In contrast to **2**, no cleavage of the DMSO ligand was detected for **1**. Additionally, **4** features a small mass signal corresponding to [4 – CH₃]⁺ (*m/z* 507.05), which may indicate that the reaction pathway for this compound occurs via hydrolysis of the methylato and not the PTA ligand. Tandem mass spectrometric investigation by collisional activation of [1 + OH]⁺ indicated that H₂O, MeOH, and DMSO cleaved off and supports the

notion of an associative pathway or even migratory insertion into the Pt–Me bond (Figure S2).

Reactivity toward Biomolecules. The main mode of action of Pt anticancer drugs responsible for their therapeutic effect is DNA targeting.⁶¹ However, even the very well-studied mechanism of action of cisplatin seems not to be fully established yet due to the numerous potential reaction partners inside a cell.⁶² Therefore, understanding the interactions of metal-based drugs with biomolecules, such as amino acids, proteins, and nucleotides, on a molecular level is of particular interest to elucidate the reaction pathways of metal-based anticancer agents. The determination of drug–biomolecule adducts can be performed by a number of analytical methods,⁶³ and ESI-MS proved to be a reliable method for monitoring these interactions.^{64–66} The reactivity of **1**, **2**, and **4** toward selected amino acids (L-cysteine [Cys], L-histidine [His], L-methionine [Met], and L-glutamic acid [Glu]) and the model proteins ub and cyt was evaluated by means of ESI-MS (Figures S2 and S3, Tables S4–S6).

Amino Acids. Compounds **1**, **2**, and **4** were incubated with an equimolar mixture of the amino acids Met, Cys, His and Glu in water (Figure 3, Table S4). Compound **2** preferentially

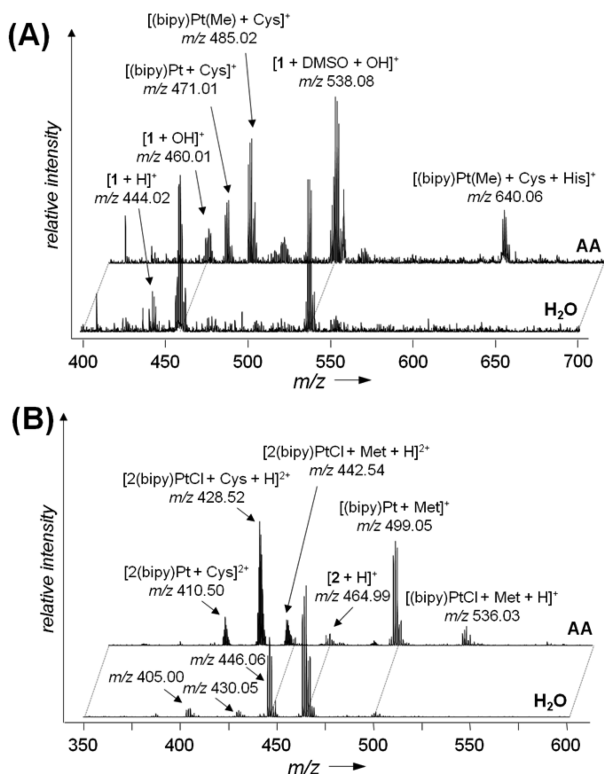


Figure 3. ESI-IT mass spectra of **1** (A) and **2** (B) after 2 h incubation in water and in the presence of a mixture of Cys/His/Met/Glu (AA) at an equimolar ratio.

formed adducts with Met and Cys, whereas His adducts were detected only after 24 h and no adducts with Glu were observed over the time of the experiment. The formation of Met and Cys adducts occurred via exchange with DMSO as indicated by the detection of the ions $[(\text{bipy-}\kappa^2\text{N,C})\text{PtCl} + \text{Met} + \text{H}]^+$ (m/z 536.03) and $[(\text{bipy-}\kappa^2\text{N,C})\text{PtCl} + \text{His} + \text{H}]^+$ (m/z 542.03). This is followed by the cleavage of the Pt–Cl bond and subsequent formation of complexes with amino acids bound in a bidentate manner, that is, $[(\text{bipy-}\kappa^2\text{N,C})\text{Pt} + \text{Met}]^+$

(m/z 499.05) and $[(\text{bipy-}\kappa^2\text{N,C})\text{Pt} + \text{His}]^+$ (m/z 505.07). Furthermore, the coordination of Met or Cys to a Pt–(bipyridine) fragment may lead to dimerization as observed, for example, as $[(\text{bipy})_2\text{Pt}_2(\mu\text{-S-Cys})]^{2+}$ (m/z 410.50) and most probably involves thiolate or thioether bridging of two Pt centers.

Compounds **1** and **4** demonstrated comparable aqueous chemistry and were less reactive toward amino acids than the kinetically more labile **2**. Interestingly, their preferences for adduct formation with amino acids were markedly different (Figure 4). Compound **1** mainly formed adducts with Cys by cleavage of the Pt–DMSO bond to yield $[(\text{bipy-}\kappa^2\text{N,C})\text{Pt}(\text{Me}) + \text{Cys} + \text{H}]^+$ (m/z 485.02) with a subsequent cleavage of the Pt–Me bond forming a bidentate adduct $[(\text{bipy-}\kappa^2\text{N,C})\text{Pt} + \text{Cys}]^+$ (m/z 471.01). However, in the mass spectra of the reaction mixture with the PTA complex **4**, the most abundant signal was attributed to adducts with His (Figure S2), which were obtained solely by cleavage of the Pt–CH₃ bond, for example, $[(\text{bipy-}\kappa^2\text{N,C})\text{Pt}(\text{PTA}) + \text{His}]^+$ (m/z 662.13) and $[(\text{bipy-}\kappa^2\text{N,C})\text{Pt}(\text{PTA}) + \text{His} + \text{H}_2\text{O}]^+$ (m/z 680.18), which is in accordance with the hydrolysis studies, while neither adducts with Glu nor Met were detected. Although possessing the same chelating ligand, the three complexes formed quite distinct adducts with amino acids depending on the nature of the monodentate ligands, that is, **2** forms adducts with Met and Cys, while **1** binds preferentially to Cys and **4** to His and Cys. This implies that the choice of the leaving group and the additional monodentate ligand influences the selectivity of the metaldrug toward certain biological nucleophiles, that is, imines, thiolates, or thioether.

The reactivity of **4** toward His and Met was also studied by $^{31}\text{P}\{^1\text{H}\}$ NMR spectroscopy. For this purpose, 2 equiv of the respective amino acid were added to a 5% [D6]DMSO/D₂O solution of **4**, and the reaction progress was determined after 30 min, 3, 24, 48 h, and 8 d. Within the first 3 h of incubation, **4** did not react with the amino acids, but after 24 h a small percentage (ca. 5%) of complex underwent ligand exchange reactions with Met, while no reaction was observed with His during this time period as shown in both ^1H and $^{31}\text{P}\{^1\text{H}\}$ NMR spectra. After 24 h of reaction of **4** with Met and His (Figures S4 and S5), the $^{31}\text{P}\{^1\text{H}\}$ NMR spectrum showed a signal at ca. –3 ppm in addition to a signal for PTA in the intact complex at –61 ppm. However, these species account for <10% of the original compound within the first 72 h, indicating high stability of **4**. The adduct formation kinetics in these experiments was higher for Met than for His.

Proteins. Compounds **1**, **2**, and **4** were incubated with a mixture of ub and cyt, and their reactions were monitored by ESI-IT-MS (Figure 5, Table S5) and ESI-TOF-MS (for a discussion of the latter compare the Supporting Information; Table S6, Figure S3). The chlorido complex **2** forms aqua species, and this resulted in the detection of pronounced Pt(bipy) adducts with both ub and cyt. In contrast, the methylate analogue **1** demonstrated some selectivity toward cyt ($[\text{cyt} + (\text{bipy})\text{Pt}(\text{OCH}_3)]^+$, m/z 12737.7), while adducts with ub were not observed. On the other hand, **4** featured only an ub adduct corresponding to $[\text{ub} + (\text{bipy-}\kappa^2\text{N,C})\text{Pt}(\text{PTA})]^+$ (m/z 9071.9). It seems that modulation of the monodentate ligands from chlorido to methylato influences the selectivity of binding toward model proteins similarly to amino acids. In general, **2** was most reactive toward ub and cyt, followed by the methylato-containing **1** and **4**. A bidentate binding mode to proteins leads to metalation of both proteins and also bis-

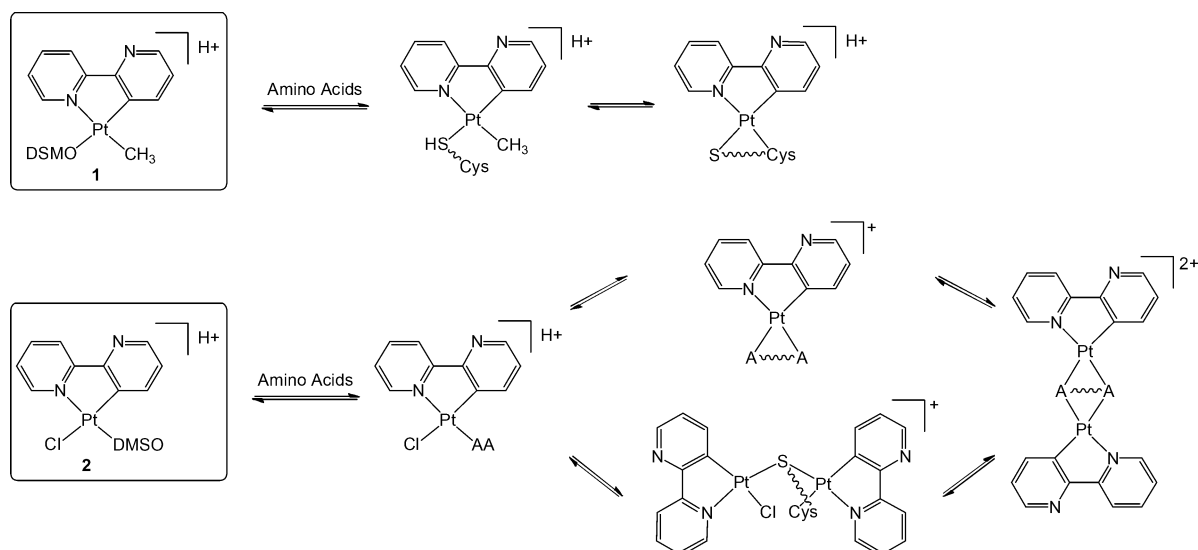


Figure 4. Reaction pathways of **1** and **2** with amino acids are displayed showing the detected ions during ESI-IT-MS analysis of the incubation mixtures.

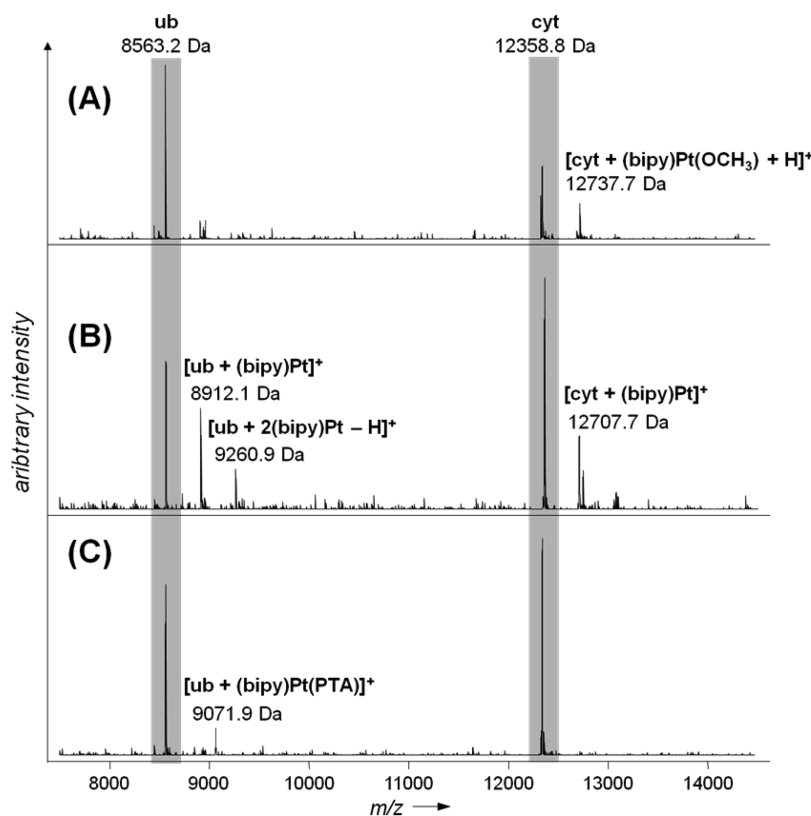


Figure 5. Deconvoluted ESI-IT mass spectra recorded in the binding studies of **1** (A), **2** (B), and **4** (C) after incubation with a ub/cyt mixture in aqueous solution for 24 h.

adducts, while monodentate binding yields only monoadducts and a certain selectivity depending on the monodentate ligand. Consequently, **1** forms adducts with cyt, while the PTA-containing **4** yields mainly ub adducts.

Cytotoxicity in Human Cancer Cell Lines. The rollover cyclometalated Pt(II) complexes were screened for their antiproliferative activity in ovarian teratocarcinoma CH1(PA-1), colon carcinoma SW480 and HCT116, and non-small cell lung cancer A549 cells by means of the colorimetric MTT

assay. The IC_{50} values are listed in Table 2. The yield of **6** was unsatisfactory, and the dinuclear compounds **7–9** were not sufficiently soluble in aqueous media to include them into biological assays.

Cisplatin was more cytotoxic than complexes **1–5** in all cell lines with the exception of SW480 where **5** was slightly more active. The antiproliferative activity of the investigated complexes in HCT116 cells decreased in the order $3 \geq 4 > 5 > 1 > 2$, whereas in other cell lines it was found to decrease in

Table 2. Cytotoxicity of Pt Complexes 1–5 and Cisplatin Given as 50% Inhibitory Concentrations (IC_{50}) in CH1(PA-1) (ovarian teratocarcinoma), A549 (non-small cell lung cancer), and SW480 and HCT116 (colon carcinoma) Cells, Determined by Means of the MTT Assay after Exposure for 48 h (HCT116) or 96 h and Their Cellular Accumulation in SW480 Cells Upon 2 h of Exposure^a

	IC_{50} values \pm SD, μ M				Cellular uptake, fg Pt/cell
	A549	CH1(PA-1)	SW480	HCT116	SW480
1	129 \pm 19	27 \pm 1	44 \pm 7	88 \pm 21	357 \pm 76
2	287 \pm 20	76 \pm 12	88 \pm 13	202 \pm 45	66 \pm 14
3	15 \pm 3	4.2 \pm 0.9	5.0 \pm 0.2	25 \pm 2	266 \pm 63
4	104 \pm 8	3.4 \pm 0.3	14 \pm 1	28 \pm 9	160 \pm 32
5	13 \pm 1	3.0 \pm 0.3	1.4 \pm 0.2	51 \pm 13	n.d. ^b
cisplatin ^{66,67}	1.3 \pm 0.4	0.14 \pm 0.03	3.3 \pm 0.4	11 \pm 2	12 \pm 1

^aNote that no direct comparison should be drawn between HCT116 and the other cell lines because of the different exposure times. Values are means \pm standard deviations obtained from at least three independent experiments. ^bn.d., not determined.

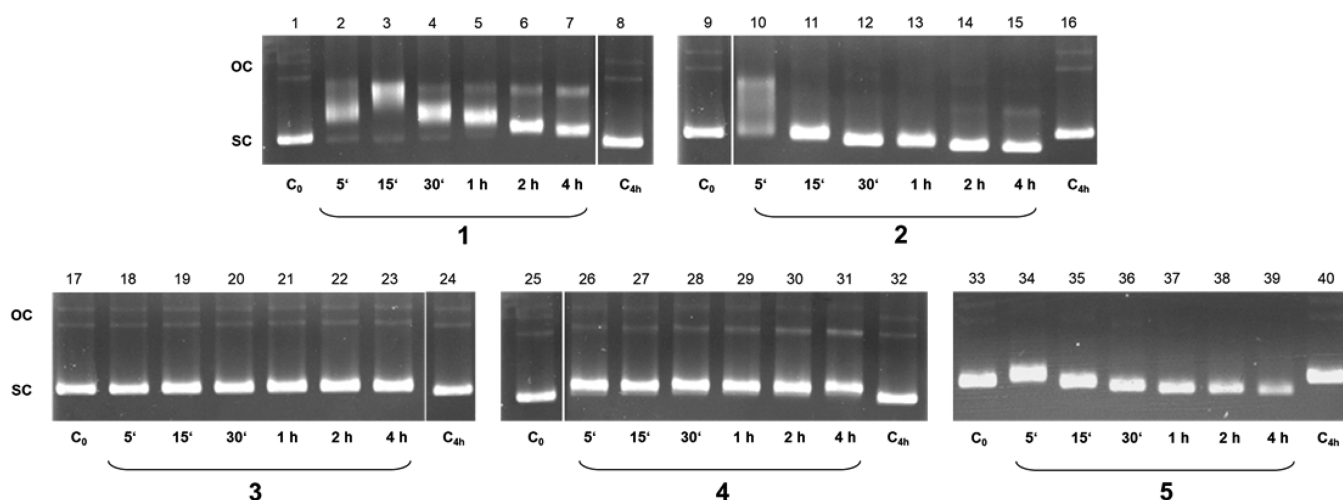


Figure 6. Electropherograms of dsDNA plasmid pUC19 after exposure to a 50 μ M solution of **1** (lanes 2–7), **2** (lanes 10–15), **3** (lanes 18–23), **4** (lanes 26–31), and **5** (lanes 34–39) for different exposure times (5 min up to 4 h) compared to untreated controls C_0 (lanes 1, 9, 17, 25 and 33) and C_{4h} (lanes 8, 16, 24, 32 and 40). SC and OC indicate supercoiled and open circular DNA, respectively. The gels for compounds **1/4** and **2/3** were run together, and the untreated controls C_0 or C_{4h} were added to the left or right of the gels, separated by a white vertical line if not directly analyzed on the adjacent lane.

the order $5 \geq 3 \geq 4 > 1 > 2$. As the incubation time for HCT116 cancer cells was only 48 h (96 h for the other cell lines), the results cannot be directly compared. Complex **2**, which was most reactive to amino acids and proteins, was the least active in all cancer cell lines and complexes with more thermodynamically stable Pt–P bonds (**3** and **4**) demonstrated higher antiproliferative activity. In SW480 and A549 cells, **5** was markedly more active than the other investigated complexes, while the PTA complexes **4** and **5** were similarly potent in the chemosensitive CH1(PA-1) cells. The biological activity of **1**, **2**, and **4** was inversely related with their reactivity toward biomolecules ($4 > 1 > 2$, where **4** was the most active and the least reactive). As observed previously for other complexes, the faster the reaction kinetics in amino acid interaction studies, the less potent are the compounds with respect to their antiproliferative activity.^{66,67} This can be compared with observations made for cisplatin, for which reactions with serum proteins have been suggested to lead to inactivation of the drug and possibly contribute to side effects experienced by patients.⁵³ However, clinical trials with cisplatin–protein adducts resulted in similar activity as cisplatin alone.⁶⁸ Interestingly, even extensive formation of Pt adducts with cellular DNA does not necessarily lead to an increase in cytotoxicity, since these adducts may be quickly removed by the

repair systems, as is the case for transplatin which was shown to be at least 2.5-fold more reactive than cisplatin with no increase of cytotoxicity.⁵⁴

Cellular Accumulation. The cellular accumulation of Pt in SW480 cells was determined by ICP-MS upon exposure to compounds **1–4** in comparison to cisplatin (Table 2). SW480 cells were chosen for the experiments because A549 cells showed the lowest sensitivity toward the tested complexes, and CH1(PA-1) cells are known to detach easily during the washing steps required in the cellular uptake experimental protocol.⁵⁶ The cellular accumulation of all tested complexes is markedly (up to \sim 30-fold) higher than for cisplatin, decreasing in the order $1 > 3 > 4 > 2$. With the exception of **1**, there is a correlation between the antiproliferative activity and cellular accumulation of the complexes. The cellular accumulation of **2** was significantly lower than that of the other compounds, which is in line with its lowest activity in this cell line ($IC_{50} = 88 \mu$ M). The triphenylphosphine complex **3** demonstrated enhanced intracellular accumulation (and higher cytotoxicity except in CH1(PA-1) cells) in comparison with the structurally similar PTA complex **4** (266 ± 63 fg Pt/cell and 160 ± 32 fg Pt/cell, correspondingly) which might be related to the higher lipophilicity of triphenylphosphine.

DNA Binding. DNA is considered the critical cellular target for Pt complexes, and changes in the tertiary DNA structure are determined by the type of adducts formed. In order to estimate the influence of the DNA adducts formed with the investigated complexes on the tertiary structure, DNA unwinding experiments were conducted. The time-dependent ability of 1–5 to modify the electrophoretic mobility of the supercoiled pUC19 plasmid DNA was determined by means of an agarose gel mobility shift assay (Figure 6).⁶⁹ The complexes were incubated at a concentration of 50 μM with pUC19 plasmid DNA at 37 $^{\circ}\text{C}$ for 5 min up to 4 h and analyzed by electrophoresis in native agarose gels. The mobility of DNA fragments migrating in the gel is influenced by the conformation of the DNA molecule. Supercoiled DNA (SC) is smaller in size, and therefore it experiences less resistance from the gel and migrates faster than open circular DNA (OC). Adducts that induce lower mobility of SC DNA relieve torsional stress by unwinding and relaxing the compact SC form. In contrast, higher mobility of OC DNA indicates the formation of adducts causing DNA condensation.⁴⁹

Based on the structures of the Pt complexes and the amino acid/protein reactivity studies, we anticipated that the Me complexes 1, 3, and 4 would be less reactive toward DNA plasmid than the kinetically more labile chlorido complexes 2 and 5. Indeed, complexes 3 and 4 induced no or minor changes in the DNA mobility within the incubation period, while 1, 2, and 5 significantly affected the electrophoretic mobility of pUC19 plasmid DNA, suggesting conformational changes and the alteration of super helicity of the DNA molecules. Complexes 1, 2, and 5 induced relaxation (unwinding) of the SC form, and at least complexes 1 and 2 induced mobilization (condensation) of the OC form of the DNA plasmid within 5 min of incubation (lanes 2 and 10). The less reactive Me/DMSO complex 1 converted plasmid DNA into a “relaxed-like” form with an apparent maximum after 15 min, which may indicate counter-coiling in the opposite direction (i.e., positive instead of negative supercoils) at later time points. It should be noted that in case of 5, the maximum unwinding may have happened too quickly to notice in this assay. Longer incubation times with 2 and 5 resulted in a higher mobility of the plasmid than for the respective controls, which probably indicates enhanced coiling. Similar patterns were observed for other Cl/DMSO–Pt^{II} complexes.^{37,39,70} It was reported that relaxation of SC form of DNA by Pt complexes was associated with local untwisting at the sites of adducts consistent with the formation of monofunctional adducts.⁵² On the contrary, condensation of the OC form was associated with the formation of multiple rigid or flexible DNA bends, caused by bifunctional intra-strand^{50,71} or interstrand adducts (two covalent bonds),⁵¹ or pseudobifunctional adducts (one covalent bond plus hydrophobic/electrostatic interactions),⁷² and was described for cisplatin,⁴⁹ transplatin,⁴⁹ and other Pt complexes.^{52,72} Hence, the observed differences in plasmid migration upon treatment with 1, 2, and 5 might indicate the formation of mono- and/or bifunctional DNA adducts; however, this hypothesis has to be confirmed by other experimental methods.

Changes in Protein Expression. To further investigate the mode of action of the complexes, we analyzed their impact on the protein levels of signaling markers involved in cell growth arrest and cell death. We assayed the protein levels of p53, a well-known transcription factor induced by DNA damage and Pt-based drugs in cancer cells and healthy cells.^{73–75} As expected, treatment of cancer cells with

oxaliplatin (Oxa) led to a marked increase in p53 protein levels (Figure 7). Complexes 1, 4, and 5 also caused an increase

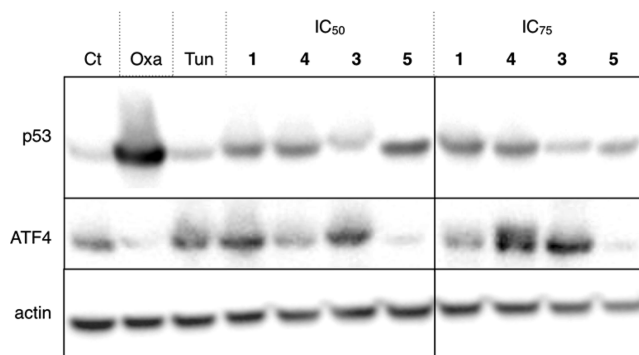


Figure 7. Protein levels for the DNA damage-induced transcription factor p53 and the ER stress-induced transcription factor ATF4. Proteins were extracted from HCT116 cells treated for 24 h using sample buffer with complexes 1, 3, 4, and 5 at their respective IC₅₀ and IC₇₅ values from MTT assay. Western blot analysis revealed p53, ATF4, and actin expression. Oxaliplatin (Oxa) and tunicamycin (Tun) were used at their IC₅₀ as positive control for DNA damage and ER stress, respectively. Ct (control) cells were not treated with any compounds.

in p53 protein level, although significantly less than oxaliplatin, while complex 3 did not affect p53 protein levels. These observations correlate with the results of DNA binding studies and suggest that complexes 1, 4, and 5 might induce DNA damage in a p53-dependent manner. Subsequently, we chose to investigate the effects of Pt(II) compounds on alternative cell death pathways not related to DNA damage, namely the endoplasmic reticulum (ER) stress pathway. The ER stress pathway is a part of the proteostasis mechanisms that control protein homeostasis of the cells in response to various stressful conditions, such as depletion in glucose, ROS production, and misfolding of proteins.⁷⁶ ER stress-inducing compounds are known to target nonapoptotic cell death pathways and might overcome multidrug resistance;⁷⁷ however, there are only few Pt-based compounds that can trigger this pathway to induce cell death.^{78–80} We chose to follow the protein levels of the transcription factor ATF4, which regulates antistress responses and is involved in PERK-eIF2 α -ATF4 pathway of ER stress process.^{81,82}

Complexes 1, 3, and 4 induced protein levels of ATF4 (Figure 7), and the strongest ATF4 upregulation was observed in cells treated with complex 3. The results suggest that complex 3 might induce p53-independent ER stress-mediated cell death. In contrast, complex 5 caused a significant diminution of ATF4 protein levels, similar to oxaliplatin, which suggests p53-dependent DNA damage as a main mode of action. Interestingly, complexes 4 and 5, that only differ by a Cl vs a Me ligand, showed drastic differential response in cancer cells. It is yet to be established whether this difference can be correlated to the stability of these two complexes and their ability to interact with biomolecules. Complex 1, which induced the strongest uncoiling of the DNA plasmid, also induced the upregulation of ATF4. These observations suggest that complex 1 is involved in more than one type of cancer cell death pathway. To conclude, despite minor variations of the ligands in complexes 1–5, they seem to display significant differences in their modes of action, as illustrated by differential impact on

purified DNA as well as on molecular signaling pathways responding to DNA damage or ER stress.

In Vivo Tests in Mouse Tumor Models. The novel Pt complexes demonstrated a mode of action drastically different from the classical Pt drug oxaliplatin. Therefore, complex **1** was subjected to *in vivo* studies with Balb/C mice. To explore its MTD, Balb/C mice were treated with **1**, and the dose of the compound was gradually increased from 4 to 15 $\mu\text{mol}/\text{kg}$. The body weight changes of the mice upon treatment are shown in Figure S6. None of the regimes caused deaths or any weight loss during the course of toxicity studies. During the whole experiment, all mice were bright, alert, and responsive.

Subsequently, the antitumor effect of the most soluble compound **1** was evaluated in comparison with oxaliplatin in the Balb/C syngeneic CT26 tumor model (Figure 8), which

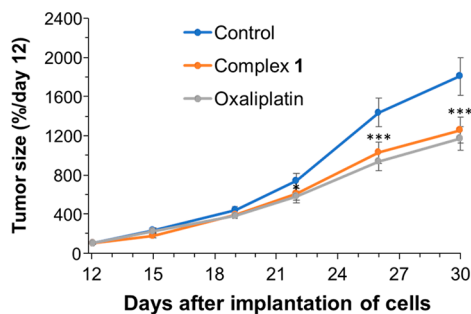


Figure 8. Growth curves of CT26 tumors starting from day 12 when tumors reached a volume of 150 mm^3 , and mice were subsequently injected with drugs of interest twice a week. Curves are means and standard deviations ($n = 8$) of tumor volume in % of tumor volume measure at day 12. Statistical analysis was carried out by the two-tail ANOVA test with Bonferroni post-test using GraphPad Prism software (GraphPad Software Inc., CA) with $P < 0.05$ considered as significant (* $p < 0.05$, *** $p < 0.001$).

respects the immune system integrity. Mouse colon cancer cells were implanted subcutaneously, and when tumors reached a size of 150 mm^3 , mice were treated intraperitoneally with oxaliplatin (25 $\mu\text{mol}/\text{kg}$) or compound **1** (18 $\mu\text{mol}/\text{kg}$) twice a week. In general, intraperitoneal administration of substances is characterized by pharmacokinetics more similar to that observed after oral administration.^{6,48} The drugs administered intraperitoneally may undergo hepatic metabolism before reaching systemic circulation, possibly resulting in a lower systemic toxicity.

Compound **1** demonstrated significant inhibition of tumor growth of about 33% compared to the control. Importantly, the effects on the tumor inhibition were similar to those caused by oxaliplatin; however, the injected dose of compound **1** (18 $\mu\text{mol}/\text{kg}$) was lower than the dose of oxaliplatin (25 $\mu\text{mol}/\text{kg}$). About half of the mice treated with compound **1** displayed signs of incontinence at the end of the treatment. Otherwise, no signs of toxicity were detected. To conclude, the *in vivo* results demonstrated that complex **1** which was suggested to inhibit cancer cell growth via several different mechanistic pathways, including DNA damage and ER stress, was shown to significantly inhibit tumor growth similar to oxaliplatin with no signs of severe toxicity. We believe the optimal therapeutic regimen is yet to be established and will be the subject of our future studies.

CONCLUSIONS

The treatment of many widespread tumor types relies heavily on cytotoxic Pt complexes. Despite their side effects and the emergence of novel therapeutic approaches (i.e., targeted therapies, immunotherapies), they remain essential parts of many therapy schemes (e.g., colon, gastric, head and neck, testicular, ovarian cancers) due to their high efficacy and low cost for health care agencies. In order to reduce the side effects of Pt compounds, a variety of strategies have been investigated. One of those is to render the complexes less labile, as for example in Pt(IV) complexes, and thereby reduce their reactivity with biomolecules, which is thought at least in part to be responsible for the side effects. In this approach, we have introduced a molecular platform based on organoplatinum compounds with a C,N-coordinated rollover 2,2'-bipyridine ligand, which were equipped with co-ligands that formed more or less stable bonds with the Pt(II) center. The small modifications of the ligand scaffold affected the overall stability of the complexes and their interactions with biomolecules. This, in turn, impacted the ability of the complexes to induce distinct pathways, such as DNA damage response and ER stress, via upregulation of p53 and ATF4, respectively. In particular, complex **3**, being the most cytotoxic derivative of the series, seems to have a completely different mode of action characterized by no impact on purified DNA or p53 protein level while presenting the strongest ability to induce ER stress by up-regulating ATF4. Excitingly, complex **1**, which induced both p53-dependent DNA-damage and a component of the ER stress response, showed similar tumor-inhibiting potency as oxaliplatin against CT26 tumors with no signs of side-effects, as indicated by no weight loss in test mice. This study illustrates how the choice of specific ligands around the metal core impacts drastically not only on the physicochemical properties of complexes in terms of reactivity but also on the molecular mechanisms triggered inside the cells, as in this case DNA damage response and ER stress.

ASSOCIATED CONTENT

Supporting Information

The Supporting Information is available free of charge on the ACS Publications website at DOI: 10.1021/acs.inorgchem.7b03210.

Crystallographic and *in vivo* data, as well as further NMR and mass spectra for stability and biomolecule interaction studies (PDF)

Accession Codes

CCDC 1585871 and 1585872 contain the supplementary crystallographic data for this paper. These data can be obtained free of charge via www.ccdc.cam.ac.uk/data_request/cif, or by emailing data_request@ccdc.cam.ac.uk, or by contacting The Cambridge Crystallographic Data Centre, 12 Union Road, Cambridge CB2 1EZ, UK; fax: +44 1223 336033.

AUTHOR INFORMATION

Corresponding Authors

*E-mail: babak.maria@nus.edu.sg.

*E-mail: c.hartinger@auckland.ac.nz; <http://hartinger.auckland.ac.nz>.

ORCID

Samuel M. Meier-Menches: 0000-0002-8930-4574

Sarah Theiner: 0000-0001-5301-0139

Muhammad Hanif: 0000-0002-2256-2317

Christian G. Hartinger: 0000-0001-9806-0893

Notes

The authors declare no competing financial interest.

ACKNOWLEDGMENTS

We thank COST actions CM1105 (short term scientific mission to M.V.B.) and BM1307, and the University of Vienna (travel award to M.V.B.) for financial support. This project was supported by the Centre National pour la Recherche Scientifique (CNRS, France; C.G.), ARC, Ligue contre le Cancer, European action. We thank Prof. Markus Galanski for providing Pt precursors.

REFERENCES

- (1) Jakupec, M. A.; Galanski, M.; Arion, V. B.; Hartinger, C. G.; Keppler, B. K. Antitumor metal compounds: more than theme and variations. *Dalton Trans.* **2008**, 183–194.
- (2) Kelland, L. The resurgence of platinum-based cancer chemotherapy. *Nat. Rev. Cancer* **2007**, *7*, 573–584.
- (3) van Zutphen, S.; Reedijk, J. Targeting platinum anti-tumour drugs: Overview of strategies employed to reduce systemic toxicity. *Coord. Chem. Rev.* **2005**, *249*, 2845–2853.
- (4) Hartinger, C. G.; Metzler-Nolte, N.; Dyson, P. J. Challenges and Opportunities in the Development of Organometallic Anticancer Drugs. *Organometallics* **2012**, *31*, 5677–5685.
- (5) Barry, N. P. E.; Sadler, P. J. Exploration of the medical periodic table: towards new targets. *Chem. Commun. (Cambridge, U. K.)* **2013**, *49*, 5106–5131.
- (6) Turner, P. V.; Brabb, T.; Pekow, C.; Vasbinder, M. A. Administration of substances to laboratory animals: routes of administration and factors to consider. *J. Am. Assoc. Lab. Anim. Sci.* **2011**, *50*, 600–613.
- (7) Wheate, N. J.; Walker, S.; Craig, G. E.; Oun, R. The status of platinum anticancer drugs in the clinic and in clinical trials. *Dalton Trans.* **2010**, *39*, 8113–8127.
- (8) Johnstone, T. C.; Park, G. Y.; Lippard, S. J. Understanding and Improving Platinum Anticancer Drugs – Phenanthriplatin. *Anticancer Res.* **2014**, *34*, 471–476.
- (9) Newkome, G. R.; Panteleo, D. C.; Puckett, W. E.; Ziefle, P. L.; Deutsch, W. A. Complexes of palladium(II), platinum(II), copper(II), cobalt(II), and zinc(II) chlorides with 6,6'-dimethyl-2,2'-dipyridyl. *J. Inorg. Nucl. Chem.* **1981**, *43*, 1529–1531.
- (10) Garelli, N.; Vierling, P. Incorporation of new amphiphilic perfluoroalkylated bipyridine platinum and palladium complexes into liposomes: stability and structure-incorporation relationships. *Biochim. Biophys. Acta, Lipids Lipid Metab.* **1992**, *1127*, 41–48.
- (11) Garelli, N.; Vierling, P. Synthesis and characterization of amphiphilic platinum and palladium complexes linked to perfluoroalkylated side-chain disubstituted bipyridines. *Inorg. Chim. Acta* **1992**, *194*, 247–253.
- (12) Edwards, G. L.; Black, D. S. C.; Deacon, G. B.; Wakelin, L. P. G. In vitro and in vivo studies of neutral cyclometallated complexes against murine leukaemias. *Can. J. Chem.* **2005**, *83*, 980–989.
- (13) Edwards, G. L.; Black, D. S. C.; Deacon, G. B.; Wakelin, L. P. G. Effect of charge and surface area on the cytotoxicity of cationic metallointercalation reagents. *Can. J. Chem.* **2005**, *83*, 969–979.
- (14) Vo, V.; Kabuloglu-Karayusuf, Z. G.; Carper, S. W.; Bennett, B. L.; Evilia, C. Novel 4,4'-diether-2,2'-bipyridine cisplatin analogues are more effective than cisplatin at inducing apoptosis in cancer cell lines. *Bioorg. Med. Chem.* **2010**, *18*, 1163–1170.
- (15) Elwell, K. E.; Hall, C.; Tharkar, S.; Giraud, Y.; Bennett, B.; Bae, C.; Carper, S. W. A fluorine containing bipyridine cisplatin analog is more effective than cisplatin at inducing apoptosis in cancer cell lines. *Bioorg. Med. Chem.* **2006**, *14*, 8692–8700.
- (16) Garelli, N.; Vierling, P.; Fischel, J. L.; Milano, G. Cytotoxic activity of new amphiphilic perfluoroalkylated bipyridine platinum and palladium complexes incorporated into liposomes. *Eur. J. Med. Chem.* **1993**, *28*, 235–242.
- (17) Klajner, M.; Hebraud, P.; Sirlin, C.; Gaiddon, C.; Harlepp, S. DNA Binding to an Anticancer Organo-Ruthenium Complex. *J. Phys. Chem. B* **2010**, *114*, 14041–14047.
- (18) Boff, B.; Gaiddon, C.; Pfeffer, M. Cancer Cell Cytotoxicity of Cyclometalated Compounds Obtained with Osmium(II) Complexes. *Inorg. Chem.* **2013**, *52*, 2705–2715.
- (19) Kaes, C.; Katz, A.; Hosseini, M. W. Bipyridine: The Most Widely Used Ligand. A Review of Molecules Comprising at Least Two 2,2'-Bipyridine Units. *Chem. Rev.* **2000**, *100*, 3553–3590.
- (20) Zucca, A.; Petretto, G. L.; Stoccoro, S.; Cinellu, M. A.; Manassero, M.; Manassero, C.; Minghetti, G. Cyclometalation of 2,2'-Bipyridine. Mono- and Dinuclear C,N Platinum(II) Derivatives. *Organometallics* **2009**, *28*, 2150–2159.
- (21) Minghetti, G.; Doppiu, A.; Zucca, A.; Stoccoro, S.; Cinellu, M. A.; Manassero, M.; Sansoni, M. Palladium(II) and platinum(II)-C(3)-substituted 2,2'-bipyridines. *Chem. Heterocycl. Compd.* **1999**, *35*, 992–1000.
- (22) Minghetti, G.; Stoccoro, S.; Cinellu, M. A.; Soro, B.; Zucca, A. Activation of a C-H Bond in a Pyridine Ring. Reaction of 6-Substituted 2,2'-Bipyridines with Methyl and Phenyl Platinum(II) Derivatives: N',C(3)-"Rollover" Cyclometalation. *Organometallics* **2003**, *22*, 4770–4777.
- (23) Cocco, F.; Cinellu, M. A.; Minghetti, G.; Zucca, A.; Stoccoro, S.; Maiore, L.; Manassero, M. Intramolecular C(sp²)-H Bond Activation in 6,6'-Dimethoxy-2,2'-Bipyridine with Gold(III). Crystal and Molecular Structure of the First N',C(3) "Rollover" Cycloaurated Derivative. *Organometallics* **2010**, *29*, 1064–1066.
- (24) Petretto, G. L.; Rourke, J. P.; Maidich, L.; Stoccoro, S.; Cinellu, M. A.; Minghetti, G.; Clarkson, G. J.; Zucca, A. Heterobimetallic Rollover Derivatives. *Organometallics* **2012**, *31*, 2971–2977.
- (25) Maidich, L.; Zuri, G.; Stoccoro, S.; Cinellu, M. A.; Masia, M.; Zucca, A. Mesoionic Complexes of Platinum(II) Derived from "Rollover" Cyclometalation: A Delicate Balance between Pt-C(sp³) and Pt-C(sp²) Bond Cleavage as a Result of Different Reaction Conditions. *Organometallics* **2013**, *32*, 438–448.
- (26) Zucca, A.; Cordeschi, D.; Maidich, L.; Pilo, M. I.; Masolo, E.; Stoccoro, S.; Cinellu, M. A.; Galli, S. Rollover Cyclometalation with 2-(2'-Pyridyl)quinoline. *Inorg. Chem.* **2013**, *52*, 7717–7731.
- (27) Maidich, L.; Zuri, G.; Stoccoro, S.; Cinellu, M. A.; Zucca, A. Assembly of symmetrical and unsymmetrical platinum(II) rollover complexes with bidentate phosphine ligands. *Dalton Trans.* **2014**, *43*, 14806–14815.
- (28) Maidich, L.; Dettori, G.; Stoccoro, S.; Cinellu, M. A.; Rourke, J. P.; Zucca, A. Electronic and Steric Effects in Rollover C-H Bond Activation. *Organometallics* **2015**, *34*, 817–828.
- (29) Fereidoonzehad, M.; Niazi, M.; Shahmohammadi Beni, M.; Mohammadi, S.; Faghhih, Z.; Faghhih, Z.; Shahsavari, H. R. Synthesis, biological evaluation, and molecular docking studies on the DNA binding interactions of platinum(II) rollover complexes containing phosphorus donor ligands. *ChemMedChem* **2017**, *12*, 456–465.
- (30) Esmaeilbeig, A.; Samouei, H.; Abedanzadeh, S.; Amirghofran, Z. Synthesis, characterization and antitumor activity study of some cyclometalated organoplatinum(II) complexes containing aromatic N-donor ligands. *J. Organomet. Chem.* **2011**, *696*, 3135–3142.
- (31) Fereidoonzehad, M.; Niazi, M.; Ahmadipour, Z.; Mirzaee, T.; Faghhih, Z.; Faghhih, Z.; Shahsavari, H. R. Cyclometalated platinum(II) complexes comprising 2-(diphenylphosphino)pyridine and various thiolate ligands: synthesis, spectroscopic characterization, and biological activity. *Eur. J. Inorg. Chem.* **2017**, *2017*, 2247–2254.
- (32) Samouei, H.; Rashidi, M.; Heinemann, F. W. Cyclometalated platinum(II) complexes containing monodentate phosphines: anti-proliferative study. *J. Iran. Chem. Soc.* **2014**, *11*, 1207–1216.
- (33) El-Mehasseb, I. M.; Kodaka, M.; Okada, T.; Tomohiro, T.; Okamoto, K.-i.; Okuno, H. Platinum (II) complex with cyclometalating 2-phenylpyridine ligand showing high cytotoxicity against cisplatin-resistant cell. *J. Inorg. Biochem.* **2001**, *84*, 157–158.

- (34) Okada, T.; El-Mehasseb, I. M.; Kodaka, M.; Tomohiro, T.; Okamoto, K.; Okuno, H. Mononuclear platinum(II) complex with 2-phenylpyridine ligands showing high cytotoxicity against mouse sarcoma 180 cells acquiring high cisplatin resistance. *J. Med. Chem.* **2001**, *44*, 4661–4667.
- (35) Fereidoonzhad, M.; Kaboudin, B.; Mirzaee, T.; Babadi Aghakhanpour, R.; Golbon Haghighi, M.; Faghhi, Z.; Faghhi, Z.; Ahmadipour, Z.; Notash, B.; Shahsavari, H. R. Cyclometalated Platinum(II) Complexes Bearing Bidentate O,O'-Di(alkyl)-dithiophosphate Ligands: Photoluminescence and Cytotoxic Properties. *Organometallics* **2017**, *36*, 1707–1717.
- (36) Frik, M.; Fernandez-Gallardo, J.; Gonzalo, O.; Mangas-Sanjuan, V.; Gonzalez-Alvarez, M.; Serrano del Valle, A.; Hu, C.; Gonzalez-Alvarez, I.; Bermejo, M.; Marzo, I.; Contel, M. Cyclometalated Iminophosphorane Gold(III) and Platinum(II) Complexes. A Highly Permeable Cationic Platinum(II) Compound with Promising Anticancer Properties. *J. Med. Chem.* **2015**, *58*, 5825–5841.
- (37) Ruiz, J.; Cutillas, N.; Vicente, C.; Villa, M. D.; Lopez, G.; Lorenzo, J.; Aviles, F. X.; Moreno, V.; Bautista, D. New Palladium(II) and Platinum(II) Complexes with the Model Nucleobase 1-Methylcytosine: Antitumor Activity and Interactions with DNA. *Inorg. Chem.* **2005**, *44*, 7365–7376.
- (38) Ruiz, J.; Lorenzo, J.; Vicente, C.; Lopez, G.; Lopez-de-Luzuriaga, J. M.; Monge, M.; Aviles, F. X.; Bautista, D.; Moreno, V.; Laguna, A. New Palladium(II) and Platinum(II) Complexes with 9-Amino-acridine: Structures, Luminescence, Theoretical Calculations, and Antitumor Activity. *Inorg. Chem.* **2008**, *47*, 6990–7001.
- (39) Ruiz, J.; Rodriguez, V.; Cutillas, N.; Espinosa, A.; Hannon, M. J. Novel C,N-chelate platinum(II) antitumor complexes bearing a lipophilic ethisterone pendant. *J. Inorg. Biochem.* **2011**, *105*, 525–531.
- (40) Ruiz, J.; Rodriguez, V.; Cutillas, N.; Lopez, G.; Bautista, D. Acetonimine and 4-Imino-2-methylpentan-2-amino Platinum(II) Complexes: Synthesis and In Vitro Antitumor Activity. *Inorg. Chem.* **2008**, *47*, 10025–10036.
- (41) Ma, D.-l.; Che, C.-M. A bifunctional platinum(II) complex capable of intercalation and hydrogen-bonding interactions with DNA: Binding studies and cytotoxicity. *Chem. - Eur. J.* **2003**, *9*, 6133–6144.
- (42) Omae, I. Applications of five-membered ring products of cyclometalation reactions as anticancer agents. *Coord. Chem. Rev.* **2014**, *280*, 84–95.
- (43) Frezza, M.; Dou, Q. P.; Xiao, Y.; Samouei, H.; Rashidi, M.; Samari, F.; Hemmateenejad, B. In Vitro and In Vivo Antitumor Activities and DNA Binding Mode of Five Coordinated Cyclometalated Organoplatinum(II) Complexes Containing Biphosphine Ligands. *J. Med. Chem.* **2011**, *54*, 6166–6176.
- (44) Vezzu, D. A. K.; Lu, Q.; Chen, Y.-H.; Huo, S. Cytotoxicity of cyclometalated platinum complexes based on tridentate NCN and CNN-coordinating ligands: Remarkable coordination dependence. *J. Inorg. Biochem.* **2014**, *134*, 49–56.
- (45) Daigle, D. J.; Pepperman, A. B.; Vail, S. L. Synthesis of a monophosphorus analog of hexamethylenetetramine. *J. Heterocycl. Chem.* **1974**, *11*, 407–408.
- (46) Romeo, R.; Scolaro, L. M. (2,2':6',2''-Terpyridine)-methylplatinum(II) chloride and (1,10-phenanthroline)-methylchloroplatinum(II). *Inorganic Syntheses*; John Wiley & Sons, Inc.: Hoboken, NJ, 1998; Vol. 32, pp 153–158.
- (47) Becker, H. *Organicum: Organic Chemistry Basic Laboratory Course*, 15th ed.; Deutscher Verlag der Wissenschaften: Berlin, 1977; p 880 pp.
- (48) Lukas, G.; Brindle, S. D.; Greengard, P. Route of absorption of intraperitoneally administered compounds. *J. Pharmacol. Exp. Ther.* **1971**, *178*, 562–566.
- (49) Cohen, G. L.; Bauer, W. R.; Barton, J. K.; Lippard, S. J. Binding of cis- and trans-dichlorodiammineplatinum(II) to DNA: Evidence for unwinding and shortening of the double helix. *Science* **1979**, *203*, 1014–1016.
- (50) Takahara, P. M.; Rosenzweig, A. C.; Frederick, C. A.; Lippard, S. J. Crystal structure of double-stranded DNA containing the major adduct of the anticancer drug cisplatin. *Nature* **1995**, *377*, 649–652.
- (51) Huang, H.; Zhu, L.; Reid, B. R.; Drobny, G. P.; Hopkins, P. B. Solution structure of a cisplatin-induced DNA interstrand cross-link. *Science* **1995**, *270*, 1842–1845.
- (52) Zorbas-Seifried, S.; Jakupec, M. A.; Kukushkin, N. V.; Groessel, M.; Hartinger, C. G.; Semenova, O.; Zorbas, H.; Kukushkin, V. Y.; Keppler, B. K. Reversion of structure-activity relationships of antitumor platinum complexes by acetoxime but not hydroxylamine ligands. *Mol. Pharmacol.* **2007**, *71*, 357–365.
- (53) Reedijk, J. Why does cisplatin reach guanine-N7 with competing S-donor ligands available in the cell? *Chem. Rev. (Washington, DC, U. S.)* **1999**, *99*, 2499–2510.
- (54) Farrell, N.; Kelland, L. R.; Roberts, J. D.; Van Beusichem, M. Activation of the trans geometry in platinum antitumor complexes: a survey of the cytotoxicity of trans complexes containing planar ligands in murine L1210 and human tumor panels and studies on their mechanism of action. *Cancer Res.* **1992**, *52*, 5065–5072.
- (55) Korch, C.; Spillman, M. A.; Jackson, T. A.; Jacobsen, B. M.; Murphy, S. K.; Lessey, B. A.; Jordan, V. C.; Bradford, A. P. DNA profiling analysis of endometrial and ovarian cell lines reveals misidentification, redundancy and contamination. *Gynecol. Oncol.* **2012**, *127*, 241–248.
- (56) Egger, A. E.; Rappel, C.; Jakupec, M. A.; Hartinger, C. G.; Heffeter, P.; Keppler, B. K. Development of an experimental protocol for uptake studies of metal compounds in adherent tumor cells. *J. Anal. At. Spectrom.* **2009**, *24*, 51–61.
- (57) Allardyce, C. S.; Dyson, P. J.; Ellis, D. J.; Heath, S. L. [Ru(η^6 -p-cymene)Cl₂(pta)] (pta = 1,3,5-triaza-7-phosphatrimethyldecane) a water soluble compound that exhibits pH dependent DNA binding providing selectivity for diseased cells. *Chem. Commun.* **2001**, 1396–1397.
- (58) Black, D. S. C.; Deacon, G. B.; Edwards, G. L. Observations on the mechanism of halogen-bridge cleavage by unidentate ligands in square planar palladium and platinum complexes. *Aust. J. Chem.* **1994**, *47*, 217–227.
- (59) Zucca, A.; Maidich, L.; Canu, L.; Petretto, G. L.; Stoccoro, S.; Cinellu, M. A.; Clarkson, G. J.; Rourke, J. P. Rollover-Assisted C(sp²)-C(sp³) Bond Formation. *Chem. - Eur. J.* **2014**, *20*, 5501–5510.
- (60) Snow, M.; Tiekink, E. Crystal structure of dichloro(N-methyl-2,2'-bipyridylium)platinum(II), C₁₁H₁₀Cl₂N₂Pt. *Z. Kristallogr.* **1992**, *198*, 148–150.
- (61) Allardyce, C. S.; Dyson, P. J. Metal-based drugs that break the rules. *Dalton Trans.* **2016**, *45*, 3201–3209.
- (62) Wexselblatt, E.; Yavin, E.; Gibson, D. Cellular interactions of platinum drugs. *Inorg. Chim. Acta* **2012**, *393*, 75–83.
- (63) Groessel, M.; Hartinger, C. G. Anticancer metallodrug research analytically painting the "omics" picture-current developments and future trends. *Anal. Bioanal. Chem.* **2013**, *405*, 1791–1808.
- (64) Hartinger, C. G.; Casini, A.; Duhot, C.; Tsybin, Y. O.; Messori, L.; Dyson, P. J. Stability of an organometallic ruthenium-ubiquitin adduct in the presence of glutathione: Relevance to antitumor activity. *J. Inorg. Biochem.* **2008**, *102*, 2136–2141.
- (65) Meier, S. M.; Tsybin, Y. O.; Dyson, P. J.; Keppler, B. K.; Hartinger, C. G. Fragmentation methods on the balance: unambiguous top-down mass spectrometric characterization of oxaliplatin-ubiquitin binding sites. *Anal. Bioanal. Chem.* **2012**, *402*, 2655–2662.
- (66) Babak, M. V.; Meier, S. M.; Legin, A. A.; Adib Razavi, M. S.; Roller, A.; Jakupec, M. A.; Keppler, B. K.; Hartinger, C. G. Am(m)ines Make the Difference: Organoruthenium Am(m)ine Complexes and Their Chemistry in Anticancer Drug Development. *Chem. - Eur. J.* **2013**, *19*, 4308–4318.
- (67) Meier, S. M.; Hanif, M.; Kandollner, W.; Keppler, B. K.; Hartinger, C. G. Biomolecule binding vs. anticancer activity: Reactions of Ru(arene)[(thio)pyr(id)one] compounds with amino acids and proteins. *J. Inorg. Biochem.* **2012**, *108*, 91–95.
- (68) Holding, J. D.; Lindup, W. E.; van Laer, C.; Vreeburg, G. C.; Schilling, V.; Wilson, J. A.; Stell, P. M. Phase I trial of a cisplatin-albumin complex for the treatment of cancer of the head and neck. *Br. J. Clin. Pharmacol.* **1992**, *33*, 75–81.

(69) Wehner, J.; Horneck, G.; Buecker, H. Plasmids as test system for the detection of DNA strand breaks. *NATO ASI Ser., Ser. A* **1993**, *243A*, 49–52.

(70) Ruiz, J.; Vicente, C.; de Haro, C.; Espinosa, A. Synthesis and Antiproliferative Activity of a C,N-Cycloplatinated(II) Complex with a Potentially Intercalative Anthraquinone Pendant. *Inorg. Chem.* **2011**, *50*, 2151–2158.

(71) Recio Despaigne, A. A.; Da Silva, J. G.; da Costa, P. R.; dos Santos, R. G.; Beraldo, H. ROS-mediated cytotoxic effect of copper(II) hydrazone complexes against human glioma cells. *Molecules* **2014**, *19*, 17202–17220.

(72) Zakovska, A.; Novakova, O.; Balcarova, Z.; Bierbach, U.; Farrell, N.; Brabec, V. DNA interactions of antitumor trans-[PtCl₂(NH₃)-(quinoline)]. *Eur. J. Biochem.* **1998**, *254*, 547–557.

(73) Benosman, S.; Gross, I.; Clarke, N.; Jochemsen, A. G.; Okamoto, K.; Loeffler, J. P.; Gaiddon, C. Multiple neurotoxic stresses converge on MDMX proteolysis to cause neuronal apoptosis. *Cell Death Differ.* **2007**, *14*, 2047–2057.

(74) Licona, C.; Spaety, M.-E.; Capuzzo, A.; Ali, M.; Santamaria, R.; Armant, O.; Delalande, F.; Dorsselaer, A. V.; Cianferani, S.; Spencer, J.; Pfeffer, M.; Mellitzer, G.; Gaiddon, C. A ruthenium anticancer compound interacts with histones and impacts differently on epigenetic and death pathways compared to cisplatin. *Oncotarget* **2017**, *8*, 2568–2584.

(75) von Grabowiecki, Y.; Abreu, P.; Blanchard, O.; Palamiuc, L.; Benosman, S.; Mériaux, S.; Devignot, V.; Gross, I.; Mellitzer, G.; Gonzalez de Aguilar, J. L.; Gaiddon, C. Transcriptional activator TAp63 is upregulated in muscular atrophy during ALS and induces the pro-atrophic ubiquitin ligase Trim63. *eLife* **2016**, *5*, e10528.

(76) Cubillos-Ruiz, J. R.; Bettigole, S. E.; Glimcher, L. H. Tumorigenic and immunosuppressive effects of endoplasmic reticulum stress in cancer. *Cell (Cambridge, MA, U. S.)* **2017**, *168*, 692–706.

(77) Chow, M. J.; Licona, C.; Pastorin, G.; Mellitzer, G.; Ang, W. H.; Gaiddon, C. Structural tuning of organoruthenium compounds allows oxidative switch to control ER stress pathways and bypass multidrug resistance. *Chem. Sci.* **2016**, *7*, 4117–4124.

(78) Wong, D. Y. Q.; Ong, W. W. F.; Ang, W. H. Induction of Immunogenic Cell Death by Chemotherapeutic Platinum Complexes. *Angew. Chem., Int. Ed.* **2015**, *54*, 6483–6487.

(79) Wang, X.; Guo, Q.; Tao, L.; Zhao, L.; Chen, Y.; An, T.; Chen, Z.; Fu, R. E platinum, a newly synthesized platinum compound, induces apoptosis through ROS-triggered ER stress in gastric carcinoma cells. *Mol. Carcinog.* **2017**, *56*, 218–231.

(80) Zou, T.; Lok, C.-N.; Fung, Y. M. E.; Che, C.-M. Luminescent organoplatinum(II) complexes containing bis(N-heterocyclic carbene) ligands selectively target the endoplasmic reticulum and induce potent photo-toxicity. *Chem. Commun. (Cambridge, U. K.)* **2013**, *49*, 5423–5425.

(81) Ye, J.; Koumenis, C. ATF4, an ER stress and hypoxia-inducible transcription factor and its potential role in hypoxia tolerance and tumorigenesis. *Curr. Mol. Med.* **2009**, *9*, 411–416.

(82) Zheng, Q.; Ye, J.; Cao, J. Translational regulator eIF2 α in tumor. *Tumor Biol.* **2014**, *35*, 6255–6264.